

We would like to thank the editor for accepting our manuscript for consideration in ACP, based our responses in the online discussion. As we already gave a very detailed response to all questions and comments from both reviewers, here we give only updated replies to the most important questions and to the handwritten comments annotated in the scanned PDF by one of the reviewers.

Reviewer comments are in red and start with “**R:**” and our replies are in black and start with “**A:**”. Original manuscript text is shown in **blue**, with new text highlighted in **yellow**.

With this response, we are also attaching 1) an annotated version of the manuscript indicating all changes; and 2) the updated manuscript.

=====

Most important concerns from reviewer #1

R4: The paper would be greatly enhanced by making a more quantitative effort to explain their data. For example, instead of speculating on the sources of moisture for the cirrus in different seasons, a more convincing approach would be to run back trajectories to show the reader where the air came from.

A: We agree that giving a more quantitative explanation would strengthen our paper. Following the referee’s suggestion, we did 24-h back-trajectory analysis using Hysplit forced by GDAS winds (0.5 deg resolution), starting from the time and altitude of each detected cirrus layer. Below is the updated figure 3 in the manuscript. The result is quite interesting as it reveals that many trajectories actually don’t follow the average wind pattern. On the other hand, many trajectories come from Colombia and Venezuela, exactly where precipitation from deep convection is found (dry season). During the wet season, most trajectories point to the near-by convection. More discussion is given in section 3 of the updated manuscript.

As we mentioned before, this trajectory analysis (suggested by referee #1) indeed gives further evidence that our cirrus clouds originate from deep convection but it is not a quantitative evidence.

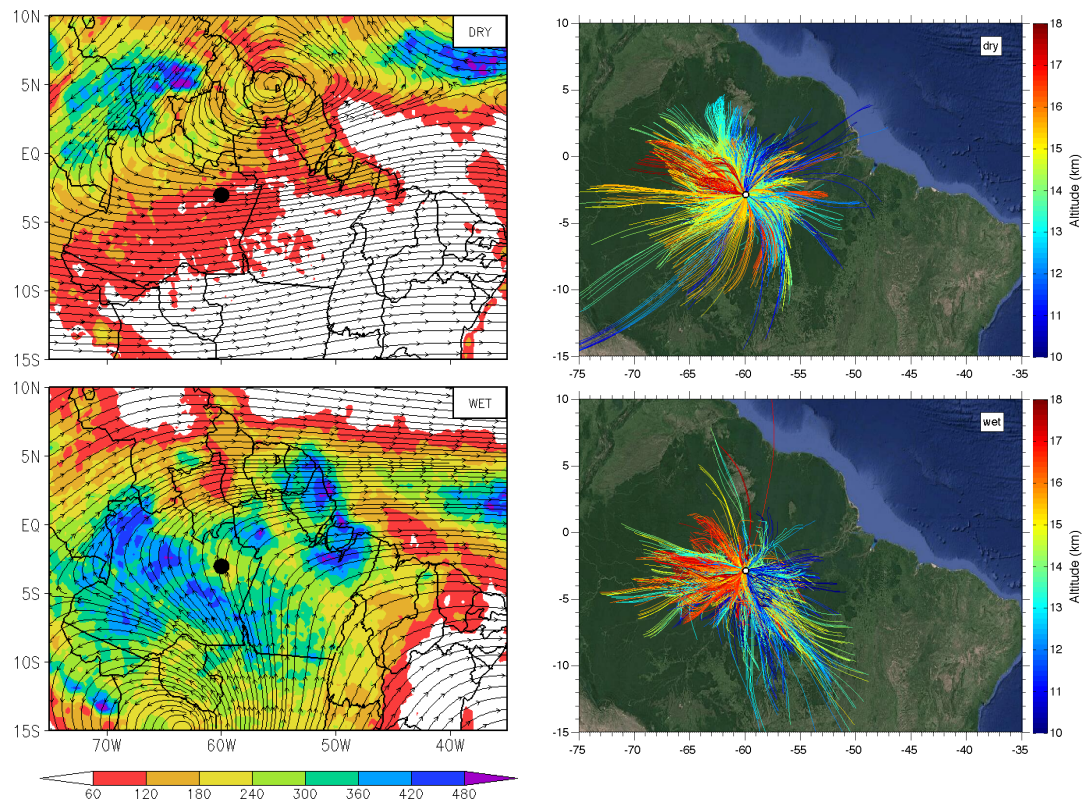


Figure 3. Left panels show mean precipitation (colors, mm/day) from the TRMM 3B42 version 7 and mean wind field (vectors, m/s) at 150 hPa from ECMWF ERA Interim reanalysis. Right panels show 24 h back trajectories of

air masses arriving at the site at the time and altitude that cirrus layers were detected. Back trajectories were computed using HYSPLIT model with 0.5° resolution winds from GDAS/NOAA. Results are shown separately for the dry (JJAS, top) and wet months (JFMA, bottom). The experimental site location is indicated in all panels.

R5: Is there reason the authors don't use the nitrogen signal to retrieve extinction? Not doing so doesn't completely discount the data presented, but it does devalue it somewhat since this paper is just another in a long-line of elastic lidar cirrus studies.

A: For our system, the weak Raman signal is only discernible from the background during nighttime, thus not being appropriate for our study, which wanted to investigate the diurnal cycle as well. Moreover, the Raman method involves calculating the derivative of the signal, which gives rise to large uncertainties in cases of such low signal-to-noise ratios as typically found at cirrus altitudes.

Besides, our experience with simulated signals have shown us that we can obtain a very precise and accurate LR with Chen's method. We did this analysis of simulated cloudy lidar profiles to evaluate the accuracy of the transmittance method but did not include in the manuscript, or in the supplement (but see discussion following your next question). We believe that these simulations and the fact that Raman methodology can in our case not be applied during daytime justify our method of choice.

R6: In addition, the transmission method is really only accurate for mid-range optical depths. Too thin and there isn't enough transmission signal to get a reliable optical depth. Too thick and there isn't enough molecular signal above the cloud. I encourage the authors to go beyond just checking the SNR above/below the cloud when doing the optical depth retrieval and to fully derive the uncertainty in the optical depth values they report. Figures 5 and 6 show optical depths down to 0.001, which I expect to be extremely uncertain when using the transmission method to retrieval optical depth.

A: We agree with the reviewer's point of view and, in fact, we have already calculated the uncertainty in all optical depth values that we have obtained. However, the plots and tables shown in the manuscript are always for averages over a huge amount of profiles, and hence we choose to report the standard deviation of the mean instead of the errors in individual retrievals.

We also agree that the COD uncertainty is very large if obtained for a single profile with COD = 0.001. In fact, we have done an extensive simulation study to validate the methods we use, which is now included as a supplement to the manuscript. For COD = 10⁻³, the relative error in a single retrieval is 120% for S/N = 50 and 1150% for SNR = 3, both large but not enough to change the cirrus category (e.g. from sub-visual to thin). Moreover, averaging over N profiles reduces this uncertainty by a factor of square-root of N. In our study, we analyzed about 37k 5-min profiles, where 21k had S/N > 3 at 12km and in 14k of these we found a cirrus cloud. Thus, the error in the mean cloud optical depth reported in Table 1, or in the histograms in figures 5 and 6, is indeed much lower, typically below 20% even for S/N = 3.

R7: The treatment and discussion of multiple scattering could be improved. Although, not explicitly stated, I'm guessing the authors use Eq. (10) from Chen et al. (2002) where eta depends on the optical depth of the cloud layer. I'd would encourage against using this equation. Chen et al. provide no physical justification (...)

A: We thank the referee for explaining the limitations of the correction proposed by Chen. To appropriately account for the multiple-scattering, we reviewed the work of Platt (1981) and Wandinger (1998) and finally decided to apply a full treatment following the model of Hogan (2008). Our new results show a change of the LR from ~16.8 sr to ~23.6 sr, while Chen's formula was giving 20.2 sr. That means that Chen's correction was indeed not valid for our case!

Reprocessing all the dataset with this more complex algorithm for multiple-scattering took much longer than anticipated and it is the main reason for the delay in submitting the updated manuscript for ACP. Nonetheless, we thank the reviewer for pushing us to do the necessary corrections.

=====

Most important concerns from reviewer #2

R1: My primary scientific concern relates to the definition of "cirrus" clouds in the manuscript. (...) In a recent paper that I authored (Campbell et al. 2015), we went to significant length to demonstrate a practical and viable definition for cirrus clouds in autonomous long-term datasets like this one, and in particular for those that lack a polarized backscatter measurement. (...)

A: We agreed with the reviewer and changed our definition to follow Campbell et al (2015). As we alerted during the online discussion, however, the amount of clouds that we no longer consider to be cirrus is less than 6%. Therefore, the numbers in the update manuscript are not so different after all. Nonetheless, a physically based definition is indeed preferred, and we thank the reviewer for the suggestion.

R2: Its unclear what the authors are saying about the presence of $\text{SNR} > 3$ in the upper troposphere with respect to cloud observation. Do they mean clear-sky? Or, do they mean within particulate scattering layers?

R4: Since the sample size is stated to relative to the ability to measure $\text{SNR} > 3$ in the upper troposphere, all of the samples appear to be relative occurrence frequencies and not absolute ones. This is HIGHLY confusing. There is no way that you're resolving an absolute cloud frequency of 67%. (...) which owes to the attenuation of the beam from low-level clouds and undersampling of the upper troposphere. (...)

R5: Speaking of this issue, nothing is said of the work of Thorsen et al. (2011) and Protat et al. (2014) and undersampling issues relating to ground-based profiling, attenuation, and the relative cloud samples that we have to analyze. This is a serious weakness that leads to three other points of concern.

A: These three questions were basically about the same issue. We apologize for not having stated it clearly in the original manuscript. As we promised in the online discussion, we modified section 2.2, removing the discussion about the SNR, and we created a new section called "frequency of occurrence and sampling issues". This is shown below.

2.4 Frequency of Occurrence and Sampling Issues

In a simplified manner, the frequency of occurrence would just be the ratio of the number of profiles with cirrus clouds to the total number of profiles. However, while one might be sure when a cirrus was detected in a given profile, there is no certainty of its presence when the profile has a low SNR or when there is no measurements. Sampling cirrus clouds with a ground-based profiling instrument might be problematic, particularly for the calculation of the frequency of occurrence, due to the obscuration by lower clouds or availability of measurements, which might introduce sampling biases (Thorsen et al., 2011).

To avoid these sampling issues, we use an approach similar to the conditional sampling proposed by Thorsen et al. (2011) and Protat et al. (2014). Firstly, we recognize that the presence of cirrus clouds is rather independent of low-level water clouds that can fully attenuate the laser beam, and independent of instrumental issues that might restrict measurement time. Hence, the best estimate of the true frequency of occurrence is the ratio of the number of profiles with cirrus, by the number of profiles where cirrus could have been detected.

These good profiles are identified as follows. The noise in each clear-sky segment of each 5-min lidar profile is evaluated. Profiles are selected if a clear-sky signal to noise ratio (SNR) higher than 3 is found at the typical cirrus altitude, and considering 7.5 m vertical resolution. This threshold was obtained from a performance evaluation of the detection algorithm and transmittance methods based on simulations for various SNR, COD and cloud thickness (not shown). What we found was that our algorithm can detect 99% of cirrus clouds with $\text{COD} > 0.005$ if the SNR is at least 3 below cloud base. In other words, given the typical cirrus cloud optical depths, the used threshold implies in a good enough SNR at cloud top for applying the transmittance method.

From the analysis of the available profiles, 20,752 were found to satisfy these criteria. July, August and September, the driest months, show the higher fraction of profiles with good SNR, while the wettest months have the lowest fraction of lidar profiles with good SNR (see figure S.1). To avoid introducing biases from the different sample sizes in different months, the frequency of occurrence for the year is calculated as the average frequency of

occurrence for each season. The frequency for each season, in turn, is calculated from the frequency of each month. Finally, the frequency for each month is calculated by averaging over the diel cycle. This is preferred than calculating the daily averages because there are more profiles with good SNR during night versus daytime.

R6: It is discussed that the lowest cloud observations occur around solar noon (10-12 LT). This leads me to believe that your instrument is suffering from issues with SNR from the bright background, even at 355 nm. Whereas it is introduced that this is potentially a real artifact, I see no reason to take such a claim at face value.

We thank the reviewer for carefully looking at all details of our results. We should say, however, that we also have looked into this minimum around solar noon to be sure that it was not a problem with the solar background. Below is the new figure 4, and the accompanying text that explain why the minimum around noon is real.

To verify that the lower cirrus cloud cover around noon was not related to a decrease in SNR and, hence, a decrease in detection efficiency, we analyzed the frequency of occurrence for different cirrus types (following Sassen and Cho, 1992). Opaque (COD > 0.3), thin ($0.3 > \text{COD} > 0.03$) and sub-visual cirrus (SVC) clouds ($\text{COD} < 0.03$) were considered. Their diurnal variation is shown in Figure 4. The larger amplitude, during both dry and wet seasons, is actually of the frequency of occurrence of opaque cirrus. During the dry (wet) season, it increases from less than 5 % (20 %) to about 30 % (50 %) in the hours following the precipitation maximum, 15 h to 19 h LT. The second larger diurnal variation is of the frequency of thin cirrus, which decreases after the sunrise from 30 % (50 %) to 20 % (30 %) during the dry (wet) season, and increase again during night time, when the opaque cirrus are dissipating. The SVC, which detection could be biased by lower SNR, do not show a clear diurnal cycle. Hence, the diurnal cycle of the frequency of occurrence of cirrus clouds in central Amazonia comes from the diurnal cycles of opaque and thin cirrus, which have a large enough COD not to be missed by the detection algorithm, even for lower SNR.

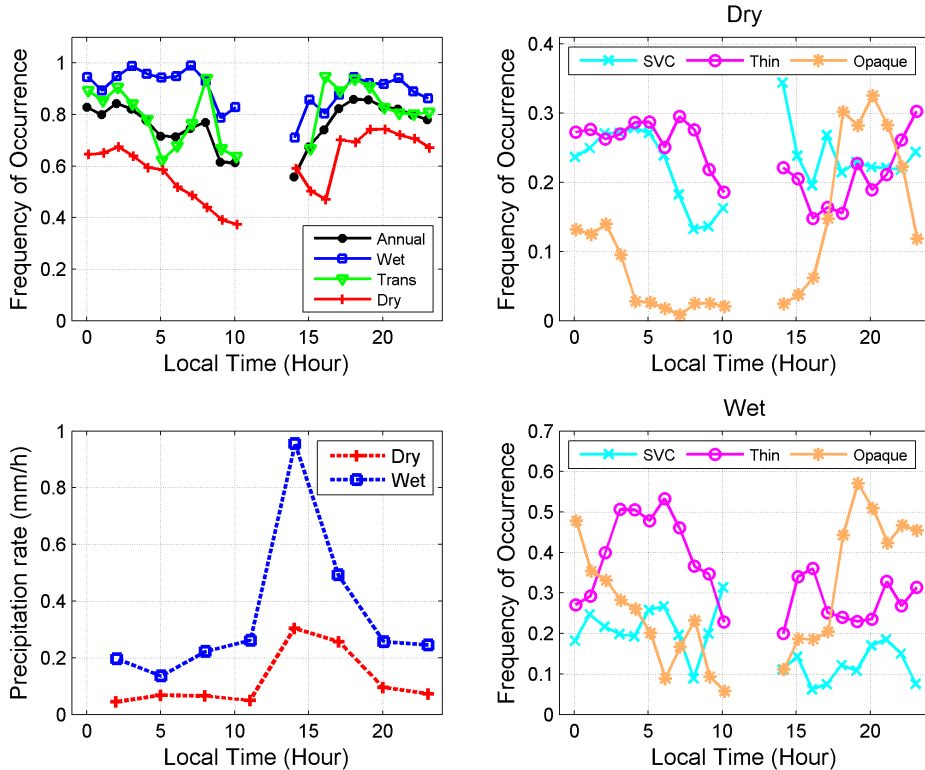


Figure 4. In the top panel, diel cycles of the hourly frequency of occurrence of cirrus clouds are shown for the annual, wet (JFMA), transition (OND), and dry (JJAS) periods. In the middle, panels show the same but for SVC, thin and opaque cirrus clouds during the dry (JJAS) and wet seasons. Lower panel shows mean observed

precipitation rate (mm/h) from TRMM version 7 over an area of $2^\circ \times 2^\circ$ centered on the site for the dry (+) and wet periods.

=====

Hand written notes by Reviewer #2

R: L. 33 – Not 30% . See Mace et al, 2007

A: Mace et al GRL 2007 used CloudSat and his paper is about hydrometeors in general, and just for one boreal summer. He says that the global average occurrence of any type of clouds is 50.6%, hence it is not possible that cirrus alone represent 40-60% as suggested by the reviewer. Sassen et al. JGR 2008 used 1-yr of Calipso + CloudSat data and found that global average cirrus coverage is 16.7%, which compares well with ISCCP data (13.2 to 19%). In a follow up study, Sassen et al JGR 2009 showed that “*about 35% of this cirrus coverage occurred within ± 15 latitude and 56% within ± 30 latitude of the equator*”.

We have modified the manuscript that now reads:

Clouds cover on average about 50 % of the Earth’s atmosphere [Mace et al., 2007] and cirrus alone cover 16.7 % (Sassen et al., 2008), with higher fractions occurring in the Tropics (Sassen et al., 2009), hence cirrus are important to understanding current climate and predicting future climate (Wylie et al. 2005, Stubenrauch et al. 2006; Nazaryan et al., 2008).

Mace, G. G., R. Marchand, Q. Zhang, and G. Stephens (2007), Global hydrometeor occurrence as observed by CloudSat: Initial observations from summer 2006, *Geophys. Res. Lett.*, 34, L09808, doi:10.1029/2006GL029017.

Sassen, K., Z. Wang, and D. Liu (2008), Global distribution of cirrus clouds from CloudSat/Cloud-Aerosol Lidar and Infrared Pathfinder Satellite Observations (CALIPSO) measurements, *J. Geophys. Res.*, 113, D00A12, doi:10.1029/2008JD009972.

Sassen, K., Z. Wang, and D. Liu (2009), Cirrus clouds and deep convection in the tropics: Insights from CALIPSO and CloudSat, *J. Geophys. Res.*, 114, D00H06, doi:10.1029/2009JD011916.

R: L53 Define Sassen and Cho 92

A: To avoid making the definition of thin and subvisible cirrus clouds too early, we modified the text that now reads:

Ground-based lidars are an indispensable tool for monitoring cirrus clouds, particularly those cirrus clouds with very low optical depth, which are undetectable by cloud radars (Comstock et al., 2002) or by passive instruments (e.g., Ackerman et al., 2008).

R: L128 – 135 What accommodation did you use for the TTL?

A: As explained in our response during the online discussion, we calculated the TTL altitude using WMO definition and the ERA Interim temperature profiles. This paragraph now reads:

Temperature, pressure, geopotential height, humidity and winds for the study period were obtained from the ERA Interim reanalysis (Dee et al., 2011) of European Center for Midrange Weather Forecast (ECMWF) with spatial resolution of 0.75° and temporal resolution of 6 h. The tropopause altitudes were obtained from ERA Interim temperature profiles over the site using the definition of the World Meteorological Organization (IMV WMO, 1966), i.e. “*the lowest level at which the lapse rate decreases to $2^\circ\text{C}/\text{km}$ or less, provided that the average lapse rate between this level and all higher levels within 2 km does not exceed $2^\circ\text{C}/\text{km}$* ”. We further assumed the lapse rate to vary linearly with pressure (McCalla, 1981), and the exact altitude where $\Gamma=2^\circ\text{C}/\text{km}$ (i.e. the tropopause) was found by linearly interpolating between the closest available pressure levels. A precipitation dataset (...)

R: L 189 – What is the absolute rate of cloud occurrence?

A: The absolute rate (i.e. number of profiles with cirrus divided by the total number of profiles measured) does not have any physical meaning (although readers may think so) and we refrain from giving that information in the paper. This absolute rate is known to be biased by low clouds, number of hours of observation, etc... (see for instance Thorsen et al, 2011 and Protat et al., 2014).

The numbers we gave at lines 193-194 are not relative numbers, as suggested by the reviewer. These are the best estimative of the true cirrus frequency. These are obtained by first excluding all profiles that do not have good clear-sky SNR at typical cirrus altitudes. We then divide the number of cirrus profiles by the total remaining. This is exactly the “conditional sampling” suggested by Thorsen et al (2011), mentioned by the reviewer.

R: L 246 – “mean temperature” is defined how? Base? Top?

A: In this case, we are giving the temperature at the altitude of the maximum backscatter. We have modified the text to make it more clear:

The mean value of the cloud maximum backscattering altitude is 13.2 ± 2.3 km and the corresponding temperature is -58 ± 17 °C.

R: L 248 – Relative frequency

A: As explained above and in the interactive discussion, absolute frequencies are just wrong and should not be reported. Moreover, our frequencies are not relative. We used the “conditional sampling” approach and, thus, they are the best estimate of the true cirrus frequency.

R: L 331 – Nucleating level

A: We thank the reviewer for the explanation. We have add it to this paragraph as follows:

As expected, there is no obvious relation of cloud top and COD. The nucleating level is independent of the vertical extent of the cloud (i.e. COD). During the dry months (...)

R: L361 Consistent with Campbell et al 2016

A: These lines now read:

The classification of cirrus clouds following Sassen and Cho (1992) shows that 40.0 % of the cirrus clouds measured in our experimental site are subvisible ($\tau < 0.03$), 37.7 % are thin cirrus ($0.03 < \tau < 0.3$) and 22.3 % are opaque cirrus ($\tau > 0.3$), which are consistent with Campbell et al. (2016). Table 2 shows (...)

R: L395 How did you derive the uncertainty?

A: Sorry for not explaining this clearly. In this case, we are just reporting the average value and the standard deviation of the distribution. The new text reads:

A mean value of 20.2 ± 7.0 (std) sr was obtained for the whole period and it varies less than 1.5 sr for different seasons. Pace et al (...)

R: L411 Why mid-level, you're likely attenuated

A: As suggested by the reviewer, we avoided analyzing base or mid-cloud temperatures. In the updated version, everything is related to cirrus top temperatures.

R: L425 Relative frequency where you had sufficient SNR

A: As discussed in the online discussion, our methodology of counting the profiles (and hence the cirrus frequency) is exactly the “conditional sampling” suggested by Thorsen et al (2011), mentioned by the reviewer. Therefore, the reported frequencies are the best estimative of the true cirrus frequency.

R: L432 SNR?

A: In our reply in the online discussion, we have shown a plot of the diurnal cycle of cirrus frequency for the different categories of cirrus. This is now the updated figure 4, which was shown above. As opaque cirrus has a very large COD (>0.3), which is well above our detection limit, the SNR cannot affect its detection. Therefore, the opaque (or even thin) cirrus marked diurnal cycle cannot be not an artifact of the sampling or of the lower SNR around noon.

1 Optical and Geometrical Properties of Cirrus Clouds in Amazonia Derived From 1-year of 2 Ground-based Lidar Measurements

3

4 Diego A. Gouveia¹, Boris Barja^{1,2,3}, Henrique M. J. Barbosa¹, Patric Seifert⁴, Holger Baars⁴, Theotonio Pauliquevis⁵ and Paulo Artaxo¹.

5 ¹Applied Physics Department, Institute of Physics, University of São Paulo, São Paulo, SP, Brazil.

6 ²Atmospheric Optics Group of Camagüey, Meteorological Institute of Cuba, Cuba.

7 ³Atmospheric Research Laboratory, University of Magallanes, Punta Arenas, Chile.

8 ⁴Leibniz Institute for Tropospheric Research (TROPOS), Leipzig, Germany

9 ⁵Department of Environmental Sciences, Federal University of São Paulo, Diadema, SP, Brazil.

10

11 Correspondence to: Boris Barja Gonzalez (bbarja@gmail.com)

12 **Abstract.** Cirrus clouds cover a large fraction of tropical latitudes and play an important role in Earth's radiation budget. Their optical properties, altitude, vertical and
13 horizontal coverage control their radiative forcing, and hence detailed cirrus measurements at different geographical locations are of utmost importance. Studies reporting
14 cirrus properties over tropical rain forests like the Amazon, however, are scarce. Studies with satellite profilers do not give information on the diurnal cycle, and the satellite
15 imagers do not report on the cloud vertical structure. At the same time, ground-based lidar studies are restricted to a few case studies. In this paper, we derive the first
16 comprehensive statistics of optical and geometrical properties of upper-tropospheric cirrus clouds in Amazonia. We used one year (July 2011 to June 2012) of ground-based
17 lidar atmospheric observations north of Manaus, Brazil. This dataset was processed by an automatic cloud detection and optical properties retrieval algorithm. Upper-
18 tropospheric cirrus clouds were observed more frequently than reported previously for tropical regions. The frequency of occurrence was found to be as high as 88% during
19 the wet season and not lower than 50% during the dry season. The diurnal cycle shows a minimum around local noon and maximum during late afternoon, associated with
20 the diurnal cycle of precipitation. The mean values of cirrus cloud top and base heights, cloud thickness and cloud optical depth were 14.3 ± 1.9 (std) km, 12.9 ± 2.2 km,
21 1.4 ± 1.1 km, and 0.25 ± 0.46 , respectively. Cirrus clouds were found at temperatures down to -90°C . 6 % of the Cirrus clouds were above the base of the tropical tropopause
22 layer. The vertical distribution was not uniform, and thin and subvisible cirrus occurred more frequently closer to the tropopause. The mean lidar ratio was 23.3 ± 8.0 sr.
23 However, for subvisible cirrus clouds a bimodal distribution with a secondary peak at about 44 sr was found suggesting a mixed composition. A dependence of the lidar ratio

Henrique de Melo J..., 1/10/2017 5:14 PM

Deleted: Theotonio Pauliquevis⁴

Henrique de Melo J..., 1/10/2017 5:14 PM

Deleted: (USP),

Henrique de Melo J..., 1/10/2017 5:14 PM

Deleted: ³Department of Natural and Earth

Henrique de Melo J..., 1/10/2017 5:14 PM

Deleted: For...one year (, from ...uly 2011 ... [1]

64 with cloud temperature (altitude) was not found, indicating that the clouds are vertically well mixed. The frequency of occurrence of cirrus clouds classified as subvisible ($\tau < 65 0.03$) were 41.6%, whilst 37.8% were thin cirrus ($0.03 < \tau < 0.3$) and 20.5% opaque cirrus ($\tau > 0.3$). Hence, in central Amazonia not only a high frequency of cirrus clouds 66 occurs, but also a large fraction of subvisible cirrus clouds. This high frequency of subvisible cirrus clouds may contaminate aerosol optical depth measured by sun- 67 photometers and satellite sensors to an unknown extent.

Henrique de Melo J..., 1/10/2017 5:14 PM
Deleted: thus ...ndicating that the cloudsth... [2]

68 1. Introduction

69 Clouds cover on average about 50% of the Earth's surface (Mace et al., 2007) and cirrus alone cover 16.7% (Sassen et al., 2008), with higher fractions occurring in the 70 Tropics (Sassen et al., 2009). Hence cirrus are important to understand current climate and to predict future climate (Wylie et al. 2005, Stubenrauch et al. 2006; Nazaryan et 71 al., 2008). Several studies emphasize the important role that cirrus clouds play in the Earth's radiation budget (i.e. Liou 1986; Lynch et al. 2002; Yang et al. 2010a). Their 72 role is twofold. First, cirrus clouds increase warming by trapping a portion of infrared radiation emitted by the Earth/atmosphere system. Second, cirrus clouds cool the 73 atmosphere by reflecting part of the incoming solar radiation back into space. The contribution of each effect and the net effect on the radiative forcing depends strongly on 74 cirrus cloud optical properties, altitude, vertical and horizontal coverage (Liou 1986, Kienast-Sjögren et al. 2016). Therefore, understanding their properties is critical to 75 determine their impact on planetary albedo and greenhouse effects (Barja and Antuña, 2011, Boucher et al., 2013). Also, tropical cirrus clouds could influence the vertical 76 distribution of radiative heating in the tropical tropopause layer (e.g., Yang et al., 2010b; Lin et al., 2013). Noticeably, it has been shown that an accurate representation of the 77 cirrus vertical structure in cloud radiative studies improved the results of these calculations (Khvorostyanov and Sassen, 2002; Hogan and Kew, 2005; Barja and Antuña, 78 2011). Recent research also shows that an increase of stratospheric water vapor is linked mainly to the occurrence of cirrus clouds in the tropical tropopause layer (TTL) 79 (Randel and Jensen, 2013). Finally, measurements of the properties of cirrus clouds at different geographical locations are of utmost importance, potentially allowing for 80 improvements in numerical model parameterizations and, thus, reducing the uncertainties in climatic studies.

Henrique de Melo J..., 1/10/2017 5:14 PM
Deleted: Cirrus clouds...cover on average ... [3]

81 Ground-based lidars are an indispensable tool for monitoring cirrus clouds, particularly those cirrus clouds with very low optical depth, which are undetectable for cloud 82 radars (Comstock et al., 2002) or for passive instruments (e.g., Ackerman et al., 2008). For this reason, several studies with ground-based lidars have reported the 83 characteristics of cirrus clouds around the globe during the last decade. There are some long-term studies reporting climatologies at midlatitudes (eg. Sassen and Campbell, 84 2001; Goldfarb et al., 2001; Giannakaki et al., 2007; Hoareau et al., 2013; Kienast-Sjögren et al. 2016) and tropical regions (eg. Comstock et al., 2002; Cadet et al., 2003; 85 Antuña and Barja, 2006; Seifert et al., 2007; Thorsen et al., 2011; Pandit et al., 2015). Table 1 shows an overview of these studies with different values for cirrus clouds 86 characteristics in diverse geographical regions. There are also some short-term reports on cirrus clouds characteristics during measurement campaigns at midlatitudes (e.g. 87 Immler and Schrems, 2002a) and tropical latitudes (Immler and Schrems, 2002b, Pace et al., 2003 and references therein). Additionally, satellite-based lidar measurements 88 have been used to investigate the global distribution of cirrus characteristics (eg. Nazaryan et al., 2008; Sassen et al., 2009; Sassen et al., 2009; Wang and Dessler 2012, Jian

Henrique de Melo J..., 1/10/2017 5:14 PM
Deleted: identifying optically thin and ... [4]

125 et al., 2015). Characteristics of tropical and subtropical cirrus clouds have similar geometrical values and they occur at higher altitudes than those at midlatitudes. However,
126 the frequencies of occurrence of cirrus cloud types differ significantly between different locations.
127 Reports on cirrus cloud measurement over tropical rain forests like in Amazonia are scarce. Just a few global studies with satellite instruments include these regions, and they
128 do not provide information on the daily cycle. There are also a few studies focused on deep convection in Amazonia that reported cirrus clouds (eg. Machado et al., 2002;
129 Hong et al., 2005; Wendisch et al., 2016), but no lidar measurements were used. Baars et al. (2012) focused on aerosol observations with a ground-based Raman lidar, and
130 thus report exemplary only one cirrus cloud case that was observed between 12 km and 16 km height on September 11, 2008 during the 11-months measurement period in
131 2008. Barbosa et al. (2014) describe a week of cirrus cloud measurements performed from 30 August to 6 September 2011 during an intensive campaign for calibration of the
132 water vapor channel of the UV Raman lidar, which is also used in this study. Cirrus clouds during that period were present in 60% of the measurements. Average base and top
133 heights were 11.5 km and 13.4 km, respectively, and average maximum backscatter occurred at 12.8 km. Most of the time, two layers of cirrus clouds were actually found.
134 From the above discussion, the importance of continuous and long-term observations of tropical cirrus clouds is evident. In the present study, we use one year of ground-
135 based lidar measurements (July 2011 to June 2012) at Manaus, Brazil to investigate the seasonal and daily cycles of geometrical (cloud top and base altitude) and optical
136 (cloud optical depth and lidar ratio) properties of cirrus over a tropical rain forest site. In section 2, a description of the Raman lidar system, dataset, processing algorithms and
137 site are given. The results and discussion are presented in section 3. We close this paper with concluding remarks in section 4.

138 2. Instrumentation, dataset and algorithms.

139 2.1. Site and instrument description

140 The ACONVEX (Aerosols, Clouds, cONvection EXperiment) or T0e (nomenclature of the GoAmazon2014/15 experiment, Martin et al. 2016) site is located up-wind from
141 Manaus-AM, Brazil, at 2.89° S and 59.97° W, in the central part of the Amazon Forest, as shown in the satellite image of Figure 1. Atmospheric observations at this site
142 began in 2011 with the objective to operate a combination of several instruments for measuring atmospheric humidity, clouds and aerosols as well as processes which lead to
143 convective precipitation (Barbosa et al., 2014).
144 As with most tropical continental sites, the diurnal cycle of precipitation is strong with a late afternoon peak (Adams et al., 2013). The precise definition of the climatological
145 seasons varies among authors (e.g. Machado et al., 2004; Arraut et al., 2012; Tanaka et al., 2014), however, deep convection is a characteristic of the region during all year.
146 For our site and period of study, we considered a wet (Jan-Apr), a dry (Jun-Sep), and a transition (Mar, Oct-Dec) season. Convection is more active during the wet season,
147 when the intertropical convergence zone (ITCZ) influences the region. As the ITCZ moves northward during the months of the dry month, the convective activity decreases.
148 The lidar system (LR-102-U-400/HP, manufactured by Raymetrics Advanced Lidar Systems) operates in the UV at 355 nm. Three channels detect the elastically
149 backscattered light at 355 nm as well as the Raman-scattered light of nitrogen (387 nm) and water vapor (408 nm), simultaneously in analog and photon-counting modes. The
150 system is tilted by 5° from the zenith to avoid specular reflection of horizontally oriented ice crystals (e.g., Westbrook et al., 2010). It is automatically operated 7 days a week,

Henrique de Melo J..., 1/10/2017 5:14 PM
Deleted: these values are...higher altitudes ... [5]

Henrique de Melo J..., 1/10/2017 5:14 PM
Deleted: Cirrus clouds measurements ... [6]

Henrique de Melo J..., 1/10/2017 5:14 PM
Deleted: diurnal variability...of geometrical ... [7]

Henrique de Melo J..., 1/10/2017 5:14 PM
Deleted: sites... Martin et al. 2016) site is ... [8]

Henrique de Melo J..., 1/10/2017 5:14 PM
Deleted: ...at 355 nm. Three and has also ... [9]

211 only being closed between 11 am and 2 pm local time (LT is -4 UTC) to avoid the sun crossing the field of view. Detailed information about the lidar system and its
212 characterization are given by Barbosa et al. (2014). To retrieve the particle backscatter and extinction profiles from the lidar signal, the temperature and pressure profiles were
213 obtained from the radio soundings launched at 0 and 12 UTC from the Ponta Pelada Airport, located 28.5 km to the South (3.14° S, 59.98° W) of the experimental site.

214 **2.2. Datasets**

215 The lidar dataset used in the present study comprises measurements recorded between July 2011 and June 2012. A total of 36,597 5-minute profiles were analyzed,
216 corresponding roughly to 1/3 of the maximum possible number of profiles during 1 year.
217 For the long-term analysis, winds were obtained from the ERA Interim reanalysis (Dee et al., 2011) of European Center for Midrange Weather Forecast (ECMWF) with
218 spatial resolution of 0.75° and temporal resolution of 6 h. The tropopause altitudes were calculated using ERA Interim temperature profiles interpolated to the measurement
219 time of each cirrus layer observation. We followed the definition of the World Meteorological Organization (IMV WMO, 1966), i.e. “the lowest level at which the lapse rate
220 decreases to $2^{\circ}\text{C km}^{-1}$ or less, provided that the average lapse rate between this level and all higher levels within 2 km does not exceed $2^{\circ}\text{C km}^{-1}$ ”. We further assumed the
221 lapse rate to vary linearly with pressure (McCalla, 1981), and the exact altitude where $\Gamma=2^{\circ}\text{C km}^{-1}$ (i.e. the tropopause) was found by linearly interpolating between the
222 closest available pressure levels. Precipitation was obtained from TRMM (Tropical Rainfall Measuring Mission) version 7 product 3B42 (Huffman et al., 2007) with 0.25°
223 and 3 h of spatial and temporal resolution, respectively. Back trajectories were calculated using the HYSPLIT model (Stein et al., 2015) forced by meteorological fields from
224 the US National Oceanic and Atmospheric Administration (NOAA) Global Data Assimilation System (GDAS), available at 0.5 degree resolution.

225 **2.3. Cirrus cloud detection algorithm.**

226 We used an automatic algorithm for the detection of the cloud base, the cloud top and the maximum backscattering heights, based on Barja and Aroche (2001). The algorithm
227 is explained in detail in Barbosa et al. (2014) and is in here only described briefly. Basically, it assumes a monotonically decreasing intensity of the lidar signal with altitude
228 in a clear atmosphere and searches for significant abrupt changes. These abrupt changes are marked as a possible cloud base. Examining the signal noise, each true cloud base
229 is discriminated. Then, the lowest altitude above cloud base with signal lower than that at cloud base and corresponding to a molecular gaseous atmosphere is determined as
230 the cloud top. When more than one layer is present in the same profile, and their top and base are separated more than 400 m, they are considered as individual clouds. Figure
231 S.2 gives an example of cloud detection. Barbosa et al. (2014) provide also information on the discrimination of false alarms and distinguishing aerosols from thin cloud
232 layers. After obtaining the base, top and maximum backscatter heights, the corresponding cloud temperatures are obtained from the nearest radiosonde. A detected high cloud
233 is classified as a cirrus cloud if the cloud top temperature is lower than -37°C (Sassen and Campbell, 2001; Campbell et al., 2015). These temperatures are typically found at
234 about 10.5 km height over Amazonia.

Henrique de Melo J..., 1/10/2017 5:14 PM

Deleted: between July 2011 and June 2012. A total of 36,597 5-minute profiles were analyzed and only 20,752 had a signal to noise ratio (SNR) higher than 3 at the characteristic altitudes of the possible cirrus clouds occurrence (between 8 km and 20 km). Statistical tests (not shown) were conducted ... [10]

Henrique de Melo J..., 1/10/2017 5:14 PM

Deleted: Temperature, pressure, geopoten ... [11]

Henrique de Melo J..., 1/10/2017 5:14 PM

Deleted: This dataset was used to obtain t ... [12]

Henrique de Melo J..., 1/10/2017 5:14 PM

Deleted: This

Henrique de Melo J..., 1/10/2017 5:14 PM

Deleted: and the change between the pos ... [13]

Henrique de Melo J..., 1/10/2017 5:14 PM

Deleted: cloud

Henrique de Melo J..., 1/10/2017 5:14 PM

Deleted: the

Henrique de Melo J..., 1/10/2017 5:14 PM

Deleted: algorithm

Henrique de Melo J..., 1/10/2017 5:14 PM

Deleted: details

Henrique de Melo J..., 1/10/2017 5:14 PM

Deleted: fully automated algorithm, whic ... [14]

Henrique de Melo J..., 1/10/2017 5:14 PM

Deleted: alarm

Henrique de Melo J..., 1/10/2017 5:14 PM

Deleted: is

Henrique de Melo J..., 1/10/2017 5:14 PM

Deleted: layer has a

Henrique de Melo J..., 1/10/2017 5:14 PM

Deleted: equal or below

Henrique de Melo J..., 1/10/2017 5:14 PM

Deleted: -25°C .

Henrique de Melo J..., 1/10/2017 5:14 PM

Deleted: reached above 8

Henrique de Melo J..., 1/10/2017 5:14 PM

Deleted: in our experimental site almost a ... [15]

301 2.4. Frequency of Occurrence and Sampling Issues

302 In a simplified manner, the frequency of occurrence would just be the ratio of the number of profiles with cirrus clouds to the total number of profiles. However, while one
303 might be sure when a cirrus was detected in a given profile, there is no certainty of its presence when the profile has a low signal-to-noise ratio or when there is no
304 measurement available. Sampling cirrus clouds with a ground-based profiling instrument might be problematic, particularly for the calculation of the temporal frequency of
305 occurrence, due to the obscuration by lower clouds, or availability of measurements, which might introduce sampling biases (Thorsen et al., 2011).

306 To avoid these sampling issues, we use an approach similar to the conditional sampling proposed by Thorsen et al. (2011) and Protat et al. (2014). First, we recognize that the
307 presence of cirrus clouds is rather independent of low-level liquid water clouds that can fully attenuate the laser beam, and independent of instrumental issues that might
308 restrict measurement time. Hence, the best estimate of the true frequency of occurrence is the ratio of the number of profiles with cirrus, by the number of profiles where
309 cirrus could have been detected.

310 These good profiles are identified as follows. The noise in each clear-sky bin follows a Poisson distribution and is evaluated as the square root of the signal. The signal-to-
311 noise ratio (SNR) is defined as the background corrected signal divided by the noise, similarly to Heese et al. (2010). Profiles are selected if a clear-sky SNR higher than 1.0
312 is found at 16 km, considering 7.5 m vertical resolution. Note that this is not the SNR of the cirrus cloud (cirrus – molecular / noise), which typically ranges from 6 to 36. The
313 threshold was obtained from a performance evaluation of the detection algorithm. Using simulations, we varied cloud thickness (15 m to 4.5 km), cloud backscatter
314 coefficient (1 to 10 $Mm^{-1} sr^{-1}$) and SNR (1 to 50). We found that our algorithm detects 99% of cirrus clouds with COD > 0.005. In other words, given the typical cirrus cloud
315 optical depths, the used threshold implies a sufficiently high SNR at cloud top for applying the transmittance method (described in section 2.5).

316 From the analysis of the available profiles, 16,025 were found to satisfy these criteria (see Table 2). July, August and September, the driest months, show the highest fraction
317 of profiles with good SNR, while the wettest months have the lowest fraction of lidar profiles with good SNR (see figure S.1). To avoid introducing biases from the different
318 sample sizes in different months, the frequency of occurrence for the year is calculated as the average frequency of occurrence for each season. The frequency for each
319 season, in turn, is calculated from the frequency of each month. Finally, the frequency for each month is calculated by averaging over the mean diurnal cycles (i.e. mean of
320 hourly means), because there are more profiles with good SNR during night compared to daytime.

321 2.5. Cloud Optical Depth, backscattering coefficient and lidar ratio.

322 The attenuation of the lidar signal by cirrus clouds can be obtained using the ratio of the range-corrected signal at the top and at the cloud base as described in Young (1995):

$$\frac{S(z_t)}{S(z_b)} = \frac{\beta(z_t)}{\beta(z_b)} e^{-2 \int_{z_b}^{z_t} \alpha_p(z') dz'} e^{-2 \int_{z_b}^{z_t} \alpha_m(z') dz'} \quad (1)$$

323 where z_b and z_t are the base and top height of a cirrus layer, and $S(z) = P(z)z^2$ is the range corrected signal. $\beta(z)$ and $\alpha(z)$ are the volumetric backscattering and extinction
324 coefficients, respectively, and each is the sum of a molecular (sub index m) and a particle (sub index p) contribution. Volumetric backscattering and extinction profiles from
325

Henrique de Melo J..., 1/10/2017 5:14 PM
Deleted: Cirrus
Henrique de Melo J..., 1/10/2017 5:14 PM
Deleted: profile
Henrique de Melo J..., 1/10/2017 5:14 PM
Deleted: determination.
Henrique de Melo J..., 1/10/2017 5:14 PM
Deleted:
Henrique de Melo J..., 1/10/2017 5:14 PM
Deleted: (
Henrique de Melo J..., 1/10/2017 5:14 PM
Deleted: ,
Henrique de Melo J..., 1/10/2017 5:14 PM
Deleted: clouds heights,
Henrique de Melo J..., 1/10/2017 5:14 PM
Deleted:

334 molecules were derived following Bucholtz (1995). Assuming a negligible aerosol contribution in the atmospheric layers just below and above the cirrus clouds (Young,
335 1995), we can express the transmittance factor of the lidar equation due to the cirrus layer, T^{cirrus} , as

$$336 T^{\text{cirrus}} = e^{-2 \int_{z_b}^{z_t} \alpha_p(z') dz'} = \frac{S(z_t) \beta(z_b)}{S(z_b) \beta(z_t)} e^{2 \int_{z_b}^{z_t} \alpha_m(z') dz'} \quad (2)$$

337 and the cirrus optical depth (for an example, see Figure S.2), τ^{cirrus} , as

$$338 \tau^{\text{cirrus}} = \int_{z_b}^{z_t} \alpha_p(z') dz' = -\frac{1}{2} \ln (T^{\text{cirrus}}) \quad (3)$$

339 The accuracy of this calculation depends mainly on the SNR at the cirrus cloud altitude. However, when the lidar signal is completely attenuated by the cirrus cloud (i.e. the
340 transmission factor approaches zero) it is impossible to obtain the true values of the cirrus top altitude and optical depth. The retrievals, in these cases called apparent values,
341 are necessarily underestimated and were not included in our analysis (see Table 2).

342 The backscattering coefficients of cirrus clouds were determined by the Fernald-Klett-Sasano method (Fernald et al., 1972; Klett, 1981; Sasano and Nakane, 1984) for each 5-
343 min averaged profile that have cloud and satisfied the conditions discussed in the previous section. For retrieving the extinction, the Klett method requires a predetermined
344 value for the layer-mean lidar ratio (LR), which is the ratio between the extinction and backscattering coefficient. Then, integrating the extinction coefficient from the cloud
345 base to cloud top, the cirrus cloud optical depth is obtained ($\tau_{\text{Klett}}^{\text{cirrus}}$). Following Chen et al. (2002), we estimated the value of LR for every cloud profile by iterating over a
346 range of values of LR and comparing the values of $\tau_{\text{Klett}}^{\text{cirrus}}$ with the independent value of the cirrus optical depth obtained from the transmittance method described above
347 (τ^{cirrus}). The cirrus mean lidar ratio is the one that minimizes the residue: $R(S) = (\tau_{\text{Klett}}^{\text{cirrus}} - \tau^{\text{cirrus}})^2$. We use the approach of Chen et al. (2002) instead of the Raman
348 method (Ansman et al., 2002) because our instrument can only detect the Raman scattered light at nitrogen during nighttime as Raman scattering is very weak compared to
349 the elastic scattering. Moreover, the Raman results are very noisy even during nighttime and, by analyzing simulated lidar profiles (not shown), we found that for the given
350 setup of our study (24/7 analysis of 5-min profiles) a more precise and accurate cirrus layer-mean LR can be obtained with Chen's method.

351 The Klett method assumes single scattering, but eventually the received photons could have been scattered by other particles multiple times before reaching the telescope.
352 This effect, named multiple scattering, increases the laser transmittance and decreases the real extinction coefficient values. Inversion of uncorrected signals could bias the
353 extinction, and hence the COD and LR, typically by 5-30% (Thorsen and Fu, 2015). This is particularly important at UV wavelengths, for which, a much stronger forward
354 scattering and therefore larger amounts of multiple scattering occur compared to the visible or infrared wavelengths. For this reason, we refrain from applying empirical
355 correction formulas (e.g. such as eq. 10 in Chen et al., 2002), and we perform a full treatment of multiple scattering following the model of Hogan (2008) that was also used
356 by Seifert et al. (2007) and Kienast-Sjögren et al. (2016). In our case, we assumed the effective radius of ice crystals to vary with temperature according to a climatology of
357 aircraft measurements of tropical cirrus data (Krämer et al., 2016a, 2016b). The full treatment corrects the retrieved LR by about 40%, from $16.8 \pm 5.8 \text{ sr}$ (uncorrected) to
358 $23.6 \pm 8.1 \text{ sr}$, while Chen's approach would only correct it to $20.2 \pm 7.0 \text{ sr}$. In the following sections, all cirrus optical properties (lidar ratio, extinction coefficient, and
359 optical depth) derived in the frame of this study were corrected for multiple-scattering.

Henrique de Melo J..., 1/10/2017 5:14 PM
Deleted: cloud
Henrique de Melo J..., 1/10/2017 5:14 PM
Deleted: :
Henrique de Melo J..., 1/10/2017 5:14 PM
Deleted: And
Henrique de Melo J..., 1/10/2017 5:14 PM
Deleted: :
Henrique de Melo J..., 1/10/2017 5:14 PM
Deleted: , ...e. the transmission factor ... [16]

Henrique de Melo J..., 1/10/2017 5:14 PM
Deleted: has large enough SNR above the ... [17]

Henrique de Melo J..., 1/10/2017 5:14 PM
Deleted: the
Henrique de Melo J..., 1/10/2017 5:14 PM
Deleted::

Henrique de Melo J..., 1/10/2017 5:14 PM
Deleted: $(\tau_{\text{Klett}}^{\text{cirrus}} - \tau^{\text{cirrus}})^2$.
Henrique de Melo J..., 1/10/2017 5:14 PM
Deleted: several...times before reaching t ... [18]

Henrique de Melo J..., 1/10/2017 5:14 PM
Deleted: calculation of cirrus ...ptical pro ... [19]

397 **3. Results and discussion.**

398 **3.1. Frequency of cirrus cloud occurrence.**

399 A total of 11,252 lidar profiles were recorded with the presence of cirrus clouds, yielding an average temporal frequency of cirrus cloud occurrence of 73.8 % from July 2011
400 to June 2012. Figure 2 shows the monthly frequency of occurrence of cirrus clouds, with the statistical error, and the precipitation in central Amazonia. There is a well-
401 defined seasonal cycle, with maximum values from November to April, reaching 88.1 % during the wet season, and a minimum value in August during the dry season (59.2
402 %), but with frequencies not lower than a rather high amount of 50 % (see Table 2). Moreover, the mean monthly cirrus cloud frequency follows the same seasonal cycle as
403 the accumulated precipitation, which responds to the seasonal changes of the ITCZ, and is higher from January to April, and lower from June to September (Machado et al.,
404 2002; 2014). The mean cirrus frequencies during the wet months are higher by a statistically significant amount than during dry months (notice the small standard deviation of
405 the mean despite the high variability). This result and the lack of the other possible formation mechanisms proposed in the literature (Sassen et al., 2002) suggest that deep
406 convection is the main formation mechanism for cirrus clouds in central Amazonia. Deep convective clouds generate cirrus clouds when winds in the upper troposphere
407 remove ice crystals of the top of the large convective column, generating the anvil cloud. The anvil cloud remains even after the deep convective cloud dissipates and persists
408 from 0.5 up to 3 days (Seifert et al., 2007).
409 To further investigate the role of deep convection as the main formation mechanism, the high-altitude circulation and the spatial distribution of precipitation were studied. The study
410 mean wind field at 150 hPa, approximately the mean cirrus top-cloud altitude (14.3 km, see Table 3), and the accumulated precipitation are shown in Figure 3. The study
411 period was divided into wet (January, February, March and April), dry (June, July, August and September) and transition (May, October, November and December) periods,
412 based on the accumulated precipitation. During the wet months, the South American monsoon is prevalent, and associated rain amounts range from 8 to 14 mm/day, with
413 monthly accumulates of about 300 mm. Winds at 150 hPa blow from the southeast at about 6 m/s. During the dry period, convective activity moved to the north toward
414 Colombia and Venezuela and the 150 hPa air flow is from the west, also at about 6 m/s, thus allowing cirrus clouds to be advected by 520 km or 4.5° per day. As previous
415 studies reported that tropical cirrus could be transported by thousands of kilometers (e.g. Fortuin et al., 2007), 24-h back-trajectories were calculated to investigate the
416 possible origin of the observed clouds. These are shown in the right panels of Figure 3 where one trajectory was calculated for each cirrus layer detected, with the arrival
417 height set to the height of top of the cirrus layer. Most of the trajectories are directed to the regions of maximum accumulated precipitation (left panel), which are much closer
418 to the site during the wet (~ 5°) than during the dry (~ 10°) season. This gives further evidence that cirrus clouds observed in central Amazonia are detrained anvils from
419 tropical deep convection. The backward trajectories also reveal that the high-altitude circulation is quite variable. Indeed, many backward trajectories do not follow the
420 average wind pattern and seem to point in the opposite direction of the precipitation, particularly during the dry season. One should note, however, that central Amazonia still
421 receives about 100 mm per month of precipitation in the dry season (reddish colors around the site, Figure 3) and most of it comes from mesoscale convective systems
422 (Machado et al., 2004; Burleyson et al., 2016). Hence, during the dry season, there is a mixture of near-by produced and long-range transported cirrus, in contrast to the wet
423 season, when there is always near-by convection.

Henrique de Melo J..., 1/10/2017 5:14 PM
Deleted: 13,946
Henrique de Melo J..., 1/10/2017 5:14 PM
Deleted: measured
Henrique de Melo J..., 1/10/2017 5:14 PM
Deleted: representing a
Henrique de Melo J..., 1/10/2017 5:14 PM
Deleted: 67 % of the total number of profiles with good SNR.
Henrique de Melo J..., 1/10/2017 5:14 PM
Deleted: Amazônia from July 2011 to June 2012, blue solid line
Henrique de Melo J..., 1/10/2017 5:14 PM
Deleted: annual
Henrique de Melo J..., 1/10/2017 5:14 PM
Deleted: during the months of
Henrique de Melo J..., 1/10/2017 5:14 PM
Deleted: December and March
Henrique de Melo J..., 1/10/2017 5:14 PM
Deleted: approximately 85 %,
Henrique de Melo J..., 1/10/2017 5:14 PM
Deleted: ,
Henrique de Melo J..., 1/10/2017 5:14 PM
Deleted: no
Henrique de Melo J..., 1/10/2017 5:14 PM
Deleted: 50 %. In tropical regions, the main mechanisms of cirrus clouds formation are deep convection, large-scale lifting of moist layers, orographic lifting over mountain slopes and ... [20]
Henrique de Melo J..., 1/10/2017 5:14 PM
Deleted: pattern
Henrique de Melo J..., 1/10/2017 5:14 PM
Deleted: (Figure 2, green line), maximum ... [21]
Henrique de Melo J..., 1/10/2017 5:14 PM
Deleted: and minimums during dry month ... [22]
Henrique de Melo J..., 1/10/2017 5:14 PM
Deleted: in
Henrique de Melo J..., 1/10/2017 5:14 PM
Deleted: in each month. The average mo ... [23]

483 The diurnal cycle of the frequency of cirrus clouds, shown in Figure 4, has also a close relation with the convective cycle. The frequency of occurrence, for the overall period
484 or any season, exhibits a minimum between 10 and 14 hours local time (LT). Maximum values are found between 17 and 18 LT, in the late afternoon, when values are
485 slightly higher than in the morning. This diurnal variation follows the diurnal cycle of convection, documented in the literature (e.g. Machado et al., 2002; Silva et al., 2011,
486 Adams et al. 2013), as also shown in Figure 4 as the diurnal cycle of precipitation averaged over an area of $2^\circ \times 2^\circ$ centered on the experimental site. The maximum
487 precipitation occurs between 13 and 18 LT, both during the dry and the wet seasons, which coincides with the increase in the cirrus frequency. In Figure 4, a smaller
488 amplitude of the cirrus frequency during the wet season months than during the dry season months is seen. This can be understood by analyzing the maximum precipitation
489 rates and the upper-altitude circulation (see Figure 3). When the frequency of deep convection is greater (3 times more in the wet season) and closer to the site ($\sim 5^\circ$ in the wet
490 and $\sim 10^\circ$ in the dry), the cirrus clouds, which are long-lived, get more evenly distributed during the day.
491 To verify that the lower cirrus cloud cover around noon was not related to a decrease in SNR and, hence, a decrease in detection efficiency, we analyzed the frequency of
492 occurrence for different cirrus types (following Sassen and Cho, 1992). Opaque (COD > 0.3), thin ($0.3 > COD > 0.03$) and sub-visual cirrus (SVC) clouds ($COD < 0.03$) were
493 considered. Their diurnal variation is also shown in Figure 4. The frequency of occurrence of opaque cirrus has the larger amplitude, during both dry and wet seasons. During
494 the dry (wet) season, it increases from less than 5 % (20 %) to about 30 % (50 %) in the hours following the precipitation maximum, 15 h to 19 h LT. The second larger
495 diurnal variation corresponds to the occurrence frequency of thin cirrus, which decreases after the sunrise from 30 % (50 %) to 20 % (30 %) during the dry (wet) season, and
496 increase again during night time, when the opaque cirrus clouds are dissipating. The SVC, whose detection could be biased by lower SNR, do not show a clear diurnal cycle.
497 Hence, the diurnal cycle of the frequency of occurrence of cirrus clouds in central Amazonia is likely a result of the diurnal cycles of opaque and thin cirrus, which have a
498 sufficiently high COD to not be missed by the detection algorithm.

499 3.2. Geometrical, optical and microphysical properties of cirrus clouds.

500 Table 2 shows column-integrated statistics of the properties of cirrus clouds during the one-year observational period also divided for the different seasons. On average, 1.4
501 layers of cirrus are present in each cloudy profile (1.25 during the dry, and 1.62 during the wet season). Column-integrated COD varies from 0.25 ± 0.45 in the dry season to
502 0.47 ± 0.65 in the wet season. The frequency of occurrence of opaque, thin and SVC column-integrated COD is 11.8 % (31.3 %), 23.9 % (37.9 %) and 23.3 % (18.3 %)
503 respectively in the dry (wet) season. The maximum backscattering altitude does not show a seasonal cycle, and is on average 13.4 ± 2.0 km (or -60 ± 15 °C).
504 As cirrus at different altitudes might have different origins and properties, it is more important to analyze the statistics based on the layers detected as shown in Table 3. The
505 overall mean value for the cloud base altitude is 12.9 ± 2.2 km, for the cloud top altitude 14.3 ± 1.9 km, and for the geometrical thickness 1.4 ± 1.1 km. The mean value of
506 the cloud maximum backscattering altitude is 13.6 ± 2.0 km. The differences between the mean values of the geometrical properties in the dry and wet seasons are not
507 statistically significant, except for the thickness, which changes from 1.3 km to 1.5 km, respectively. These values are similar to those reported by Seifert et al. (2007) for the
508 Maldives (4.1 °N, 73.3 °E): 11.9 ± 1.6 km (base), 13.7 ± 1.4 km (top), 1.8 ± 1.0 km (thickness), 12.8 ± 1.4 km (max. backscatter) and -58 ± 11 °C (temperature at max.
509 backscatter). Reports from subtropical regions also show similar values. Cadet et al. (2003) report for the Reunion Island (21°S, 55°E) cirrus cloud base and top altitudes of

Henrique de Melo J..., 1/10/2017 5:14 PM

Deleted: The mean wind field on the typical cirrus cloud occurrence altitude (200 hPa) and the precipitation spatial distribution during the dry and wet months from July 2011 to June 2012 are shown in the Figure 3. During wet months (Figure 3, lower panel), the site is inside the South American Monsoon region with great deep convection activity and associated rain ranging from 8 to 14 mm/day on average. Winds at 200 hPa blow from the southeast with about 20 m/s thus allowing the advection of cirrus clouds produced over other parts of the South Atlantic Convergence Zone. As the tropical cirrus can be transported by advection thousands of kilometers (Fortuin et al., 2007), we speculate that during the wet period, the cirrus clouds observed in central Amazonia are a mixture of locally produced and clouds transported by advection from other regions. During the dry period, the convection activity moved to the north over Colombia and Venezuela and the 200 hPa circulation is reversed. Hence, we speculate based on the high level circulation and precipitation, that a great contribution to the cirrus clouds observed during the dry months is the advection from the other r ... [24]

Henrique de Melo J..., 1/10/2017 5:14 PM

Deleted: the... statistics of the properties o ... [25]

Henrique de Melo J..., 1/10/2017 5:14 PM

Deleted: values... for the cloud base altitu ... [26]

623 11 km and 14 km, respectively. Antuña and Barja (2006) report for a subtropical experimental site (Camagüey, Cuba, 21.4° N, 77.9° W) cirrus cloud base and top altitudes of
624 11.63 km and 13.77 km, respectively. On the other hand, Sassen and Campbell (2001) show mean values for midlatitude cirrus cloud base and top of 8.79 km and 11.2 km,
625 respectively, which is lower than for tropical cirrus, and an average geometrical thickness of 1.81 km. Some cirrus cloud characteristics reported around the globe are shown
626 in Table 1 for comparison.

Henrique de Melo J..., 1/10/2017 5:14 PM
Deleted: to...subtropical experimental site ... [27]

627 The geometrical characteristics of the detected cirrus clouds were further examined by means of normalized histograms. Figure 5 shows the results for cloud base and top
628 height, thickness and cloud optical depth. Histograms for the wet and dry season months reveal differences. The cloud base distribution (Figure 5a) is wider during the wet
629 season. There are relatively more cirrus layers with cloud base below 12 km and above 16.5 km during the wet than during the dry season. Particularly, there is a peak
630 centered at 16.5 km during wet months, which does not exist during the dry season months. The distribution of geometrical thickness (Figure 5b) shows more cirrus layers
631 thicker than 2 km (and less thinner than that) in the wet season. The normalized histogram of COD (Figure 5d) shows relatively more cirrus layers with COD > 0.1 in the wet
632 season, and more with COD < 0.1 in the dry season. The largest differences, however, are in the cirrus cloud top altitude distribution (figure 5c). It shows two peaks in the wet
633 months, one centered at 14.25 km and second centered at 17.75 km. On the other hand, for dry months, there is only one peak centered at 15.75 km. These differences suggest
634 different cirrus types with different origins.

Henrique de Melo J..., 1/10/2017 5:14 PM
Deleted: the corresponding...optical deptl ... [28]

635 Comstock et al. (2002) proposed two different types of cirrus clouds at Nauru Island in the tropical western Pacific with oceanic conditions: one type (laminar thin cirrus)
636 with cloud base altitudes above 15 km and the other (geometrically thicker and more structured cirrus) with base altitudes below this value, with different characteristics. Liu
637 and Zipser (2005) used TRMM Precipitation Radar (PR) dataset to trace the deep convection and precipitation throughout the tropical zone, including oceans and continents.
638 The authors showed that only 1.38 % and 0.1 % of tropical convective systems, and consequently their generated cirrus clouds reached 14 km and 16.8 km of altitude,
639 respectively.

Henrique de Melo J..., 1/10/2017 5:14 PM
Deleted: : cirrus formed directly by anvil outflows from cumulonimbus clouds through local convection; in situ formation from slow large scale air ascent; or possible advection from other convective regions. Comstock et al....(2002 ... [29]

640 Considering these previous results, we suggest that the highest peak in wet months in cloud top distribution originates from convection penetrating the tropopause, located at
641 about 15.9-16.5 km, while the lowest peak is the ceiling of most tropical convection. The single peak observed during the dry months, in turn, originates from cirrus clouds
642 transported from large distances. Clouds generated by convective systems can persist in the atmosphere from hours to days if they are slowly lifted (Ackerman et al., 1988;
643 Seifert et al., 2007). Clouds that ascended and are horizontally transported by long distances are, in general, optically and geometrically thinner and found at higher altitudes
644 in the troposphere. This also explains why the geometrical thicknesses and optical depth are lower during the dry season months.

Henrique de Melo J..., 1/10/2017 5:14 PM
Deleted: peaks...in wet months in cloud t ... [30]

645 To investigate if the higher cirrus layers were indeed geometrically and optically thinner, a more in-depth analysis of the vertical distribution was performed. Figure 6 shows
646 two-dimensional histograms of cloud optical depth and cirrus occurrence vertical distribution for the wet season months (top) and dry season months (bottom). The right
647 panels show the vertical distribution of the frequency of occurrence for the three cirrus categories. During the wet months, there is more dispersion (wider range of COD for a
648 fixed altitude, and vice-versa) than in the dry months, which we speculate might be associated with the well-documented variability in the intensity of deep convection in
649 Amazonia (Machado et al., 2002; Adams et al., 2009, 2013, 2015). Indeed, it is only during the wet season that a significant fraction of cirrus is found above 16 km height,
650 and they have a COD ranging from 0.001 to 0.02. Moreover, while the distribution of opaque cirrus peaks at 12 km height in both seasons, thin cirrus and SVC shows a

Henrique de Melo J..., 1/10/2017 5:14 PM
Deleted: From the cloud base altitude histogram (Figure 5a), one can note the high values for the frequency of occurrence of cloud base heights between 8.5 km and 9.5 km during wet season. This peak is the second most frequent after the principal one centered at 12.25 km and 14.75 km. This secondary peak is a result of using the cloud-base temperature of -25 C as a criterion for defin ... [31]

788 bimodal distribution with the highest maxima above 14 km and 16 km respectively. This is associated with the overshooting convection discussed above, which occurs mostly
789 during the wet season (Liu and Zipser, 2005).

Henrique de Melo J..., 1/10/2017 5:14 PM
Deleted: around

790 To investigate the role of the tropopause capping on the cirrus vertical development, its altitude was calculated from the ERA Interim dataset for the observation time of each
791 cirrus profiles (see section 2.2 and Figures S.3a and S.3b). The tropopause mean altitudes during the wet, transition and dry periods are 16.5 ± 0.2 km, 16.3 ± 0.3 and
792 15.9 ± 0.4 , respectively. Therefore, a non-negligible fraction of the observed cirrus during the wet and dry seasons (Figure 6) occurred likely above the tropopause. Figure 7
793 shows the distribution of the distance from the cloud top and bottom to the tropopause. About 7% (19%) of the detected cirrus clouds have their cloud base (top) above the
794 tropopause during the wet season, and 5% (13%) during the dry season. Most of the cirrus cloud tops are found right below the tropopause inversion, except during the wet
795 season when they are uniformly distributed from -2 km to +0.5 km, which is associated with the variability in deep convection intensity as discussed above. During the dry
796 season, on the other hand, deep convection overshooting occurs primarily north of the equator (Figure 2 from Liu and Zipser, 2005). These cirrus that has formed around the
797 tropopause cannot last for a long time, as they cannot be adiabatically lifted above the tropopause inversion (Jensen et al., 1996). Therefore, they cannot be transported over
798 long distances and do not reach the measurement site, hence, there is only one maximum near 15 km in the distribution of cloud tops, which is just below the tropopause.

Henrique de Melo J..., 1/10/2017 5:14 PM
Deleted: .75 km. During the wet months, the cloud tops are spread from 13 km to 16 km, but all COD values occur at all altitudes...o investigate ... [32]

799 The classification of cirrus clouds following Sassen and Cho (1992) shows that 41.6% of the cirrus clouds measured in our experimental site are subvisible ($\tau < 0.03$), 37.8%
800 are thin cirrus ($0.03 < \tau < 0.3$) and 20.5% are opaque cirrus ($\tau > 0.3$). Table 3 shows these values for each season. SVC clouds have the highest (lower) fraction during dry
801 (wet) months. Opaque clouds have the highest (lowest) fraction during wet (dry) months, which is expected, as there is a predominance of newly generated clouds by deep
802 convection.

Henrique de Melo J..., 1/10/2017 5:14 PM
Deleted: The statistical characteristics of cirrus clouds above and below 14 km are shown in the Table 2. Mean values of the properties are different for these cloud types. Cirrus clouds above 14 km are geometrical and optically thinnest than clouds below 14 km. There are statistically significant differences between the properties of these two cirrus clouds types and between seasons. Also, there is a seasonal behaviour of the of these cloud types. During wet months the cirrus clouds are higher and optical and geometrically thicker than during the dry m ... [33]

803 This large fraction of optically thin and subvisible cirrus clouds over Amazonia present a challenge for using passive remote sensing from space, such as MODIS. As
804 mentioned by Ackerman et al. (2010), thin cirrus clouds are difficult to detect because of insufficient contrast with the surface radiance. MODIS only detects cirrus with
805 optical depth higher than 0.2 (Ackerman et al., 2008). Therefore, the MODIS's cloud-mask does not include 71% of cirrus clouds over Amazonia, and likewise, their
806 estimation of aerosol optical depth might be contaminated with these thin cirrus. Aerosol optical depth measurements from AERONET can also be contaminated with thin
807 cirrus clouds. Chew et al. (2011), for instance, estimated that the fraction of contaminated measurements of AERONET AOD in Singapore (1.5° N, 103.7° E) is about 0.034
808 to 0.060. The determination of the actual contamination of MODIS and AERONET aerosol products for Amazonia by thin cirrus will be the subject of a forthcoming study.

Henrique de Melo J..., 1/10/2017 5:14 PM
Deleted: columns. ...his large fraction of ... [34]

809 The different types of cirrus clouds measured in central Amazonia, with different formation mechanisms, optical depths and altitude ranges, are expect to be composed of ice
810 crystals of different shapes. One way to gain information on the crystal habits is to compute the lidar-ratio (Sassen et al., 1989). As explained in section 2, we are able to find
811 the average lidar ratio for the detected cirrus cloud layers in each profile, using an interactive approach instead of explicitly calculating the extinction from the Raman signal,
812 which would be available only during night-time.

Henrique de Melo J..., 1/10/2017 5:14 PM
Deleted: These...different types of cirrus ... [35]

813 Average values are given in Table 3 for all cirrus, and for each category. A mean value of 23.9 ± 8.0 (std) sr was obtained for the whole period and the variation is less than
814 1.5 sr for the different seasons, i.e., it does not show a seasonal cycle. For opaque, thin and SV cirrus the means are 25.7 ± 6.3 sr, 22.8 ± 7.9 sr and 21.6 ± 8.4 sr, respectively.
815 Pace et al., (2003), found a mean value of lidar ratio of 19.6 sr for the tropical site of Mahé, Seychelles. Seifert et al.(2007), also for tropical regions, report values close to

Henrique de Melo J..., 1/10/2017 5:14 PM
Deleted: The...mean value of 23.9 ± 820 ... [36]

946 32 sr. Platt and Diley, (1984) reported the value of 18.2 sr with an error of 20%. For the other latitudes, examples are given in Table 1. We note, however, that the lidar ratio
947 may vary greatly depending on the altitude and composition of cirrus clouds (Goldfarb et al., 2001), but also on the correction for multiple scattering (Platt, 1981; Hogan,
948 2008). The latter depends on the ice crystals effective radius, and the associated uncertainty can range from 20 to 60 % (Wandinger, 1998).
949

950 Although the mean LR for all seasons and categories are similar, their statistical distribution might yet reveal differences. Figure 8 shows the histograms of lidar ratio
951 corrected for multiple-scattering for the different seasons (top) and for the different categories (bottom). For all seasons, the most frequent lidar ratios are between 18 sr and
952 28 sr. There are notable differences only for different cirrus categories. The opaque cirrus distribution has a peak at 25 sr, while thin cirrus has its peak at about 21 sr, and
953 SVC at about 15 sr, with a secondary peak at 44 sr.

954 As the cirrus properties are expected to depend on altitude (e.g., Goldfarb et al., 2001), we examine the dependence of the lidar ratios with the cirrus cloud top temperature
955 (Figure 9). The plots show the mean, the median, and the interquartile distance. A slight increase in the lidar ratio values from 20 sr to 28 sr for a decrease in temperature from
956 -40 to -55 °C can be noticed during the dry period. During the wet period, the lidar ratio values are between 18 sr and 28 sr in all temperature intervals. Seifert et al. (2007)
957 and Pace et al. (2003) both show the same temperature dependence of the lidar ratio, but with different mean values of the lidar ratio. This behavior is an indication of a slight
variation in the microphysical characteristics of the observed clouds.

958 4. Conclusions.

959 One year of ground-based lidar measurements performed between July 2011 and June 2012 were used to investigate the geometrical and optical properties of cirrus clouds in
960 central Amazonia. An algorithm was developed to search through this dataset with high vertical and temporal resolution and to automatically find clouds, calculate particle
961 backscatter, and derive optical depth and lidar ratio. The frequency of cirrus cloud occurrence during the observation period was 73.8 %, which is higher than reported
962 previously in the literature for other tropical regions. Cirrus frequency reached 88.1 % during the wet months (January, February, March and April), but decreased to 59.2 %
963 during the dry months (June, July, August, and September). Analysis of high-level circulation and precipitation during the wet months indicate that near-by deep convection
964 was likely the main source of these cirrus. Whilst during the dry period, there was a mixture of near-by produced and advected clouds. Moreover, we found that the diurnal
965 cycle of the frequency of occurrence of opaque and thin cirrus shows a minimum around 12h LT and a maximum around 18h LT, following the diurnal cycle of the
966 precipitation for both seasons.

967 The geometrical, optical and microphysical characteristics of cirrus clouds measured in the present study were consistent with other reports from tropical regions. The mean
968 values were 12.9 ± 2.2 km (base), 14.3 ± 1.9 km (top), 1.4 ± 1.1 km (thickness), and 0.25 ± 0.46 (optical depth). Cirrus clouds were found at temperatures down to -90 °C. 6
969 % (16 %) of the observed cirrus had their base (top) above the tropopause level or in the tropical tropopause layer.

970 By simultaneously analyzing cloud altitude and COD, it was found that cirrus clouds observed during the dry season months are optically thinner and lower in altitude than
971 those during the wet period. During the wet season months, there is a wider range of COD for a fixed altitude, and vice-versa, which is associated with the variability in the

Henrique de Melo J..., 1/10/2017 5:14 PM
Deleted:(1984) reported the value of 1 ... [37]

Henrique de Melo J..., 1/10/2017 5:14 PM
Deleted: After the analysis of the properties of the cirrus clouds it is interesting to examine the behavior of the variable with the temperature. Figure 9 show the dependence of the geometrical thickness, optical depth and lidar ratios with the cirrus clouds temperature. The plots show temperature uniform intervals of 2.5 °C, and the variables with their mean and standard deviation for each corresponding interval. The upper and middle panels contain the dependence of the geometrical thickness and optical depth with cloud base temperature, respectively. We can see both variables increase at higher temperatures. Values nearly to 3 km of geometrical thickness and 0.9 optical depth correspond to a temperature of -25 °C, decreasing monotonically for lower temperatures in both month's periods. Similar results are reported by Hoareau et al. (2013) and Seifert et al. (2007). - ... [38]

Henrique de Melo J..., 1/10/2017 5:14 PM
Deleted: The ACONVEX site started in 2011 with the goal...of continuously monitoring clima ... [39]

Henrique de Melo J..., 1/10/2017 5:14 PM
Deleted: and in agreement ...ith other rep ... [40]

Henrique de Melo J..., 1/10/2017 5:14 PM
Deleted: Moreover,...the higher values of ... [41]

1083 intensity of deep convection in Amazonia. The vertical distribution of the frequency of occurrence of the detected clouds shows a bimodal distribution for thin and SV cirrus
1084 during the wet season, which originates from overshooting convection.

1085 For the first time, the lidar ratio of cirrus clouds was obtained for the Amazon region. The mean lidar ratio corrected for multiple-scattering was 23.6 ± 8.1 sr, in agreement
1086 with other reports from the tropical regions. The statistical distribution of lidar ratios measured during the different seasons is the same, and they also do not vary with the
1087 temperature (altitude) of the cirrus clouds, indicating that these clouds are well mixed in the vertical. It was observed, however, that the distributions of the lidar ratio for
1088 different cirrus categories are quite different. They are more skewed towards lower lidar ratios for smaller COD. From all cirrus clouds observed, 41.6% were classified as
1089 subvisible (COD < 0.03), 37.8% as thin (0.03 < COD < 0.3) and 20.5% as opaque (COD > 0.3). During the dry months, subvisible cirrus clouds reached a maximum
1090 frequency of occurrence of 46 %, while opaque cirrus have their maximum during the wet season months (25.2 %). These values are characteristic for the region under study
1091 and somewhat different from other tropical regions. Thus, central Amazonia has a high frequency of cirrus clouds in general, and a large fraction of subvisible cirrus clouds.
1092 Therefore, the aerosol optical depth determined by Sun photometers and satellite based sensors in this region might be contaminated by the presence of these thin clouds.
1093 Future work must be conducted in order to evaluate how large this contamination might be over Amazonia.

Henrique de Melo J..., 1/10/2017 5:14 PM

Deleted: same cloud base altitude are more optically thick during wet season. The ... [42]

Henrique de Melo J..., 1/10/2017 5:14 PM

Deleted: this...region. The mean lidar rati ... [43]

1094 5. Acknowledgements

1095 We thank our colleague, David K Adams from UNAM and two reviewers for reading the manuscript and giving valuable comments. We thank Martina Krämer for sharing the
1096 aircraft data on tropical cirrus. D.A.G. acknowledges the support of the CNPq fellowship program. B.B. acknowledges the financial support of CAPES project A016_2013 on
1097 the program Science without Frontiers and the SAVERNET project. H.M.J.B. and P.A. acknowledge the financial support from FAPESP Research Program on Global
1098 Climate Change under research grants 2008/58100-1, 2009/15235-8, 2012/16100-1, 2013/50510-5, and 2013/05014-0. Maintenance and operation of the instruments at the
1099 experimental site would not have been possible without the institutional support from EMBRAPA. We thank INPA, The Brazilian Institute for Research in Amazonia, and the
1100 LBA Central office for logistical support. Special thanks to Marcelo Rossi, Victor Souza and Jocivaldo Souza at Embrapa, and to Ruth Araujo, Roberta Souza, Bruno Takeshi
1101 and Glauber Cirino from LBA. The authors gratefully acknowledge the NOAA Air Resources Laboratory (ARL) for the provision of the HYSPLIT transport and dispersion
1102 model used in this publication.

Henrique de Melo J..., 1/10/2017 5:14 PM

Deleted: the researcher...David K Adams ... [44]

1103 6. References

1104 Ackerman, S., Holz, R., Frey, R., and Eloranta, E.: Cloud Detection with MODIS: Part II Validation, J Atmos Oceanic Tech, 25(1073-1086),
1105 doi:DOI:10.1175/2007JTECHA1053.1, 2008.

1152 Ackerman, S., Frey, R., Strabala, K., Liu, Y., Gumley, L., Baum, B., Menzel, P.: Discriminating Clear-Sky From Cloud With MODIS. Algorithm Theoretical Basis
 1153 Document (MOD35). ATBD Version 6.1. October 2010. 2010.

1154 Adams, D. K., Souza, E., and Costa, A.: Moist Convection in Amazonia: Implications for Numerical Modeling (in Portuguese). *Revista Brasileira de Meteorologia*, 13, 168-
 1155 178, 2009.

1156 Adams, D. K., Gutman, S. I., Holub, K. L., and Pereira, D. S.: GNSS observations of deep convective time scales in the Amazon. *Geophysical Research Letters*, 40, 2818-
 1157 2823, 2013.

1158 Adams, D. K., Fernandes, R. M. S., Holub, K. L., Gutman, S. I., Barbosa, H. M. J., Machado, L. A.T., Calheiros, A. J. P., Bennett, R. A., Kursinski, E. R., Sapucci, L. F.,
 1159 DeMets, C., Chagas, G. F. B., Arellano, A., Filizola, N., Amorim Rocha, A. A., Araújo Silva, R., Assunção, L. M. F., Cirino, G. G., Pauliquevis, T., Portela, B. T. T.,
 1160 Sá, A., de Sousa, J. M., and Tanaka, L. M. S: The Amazon Dense GNSS Meteorological Network: A New Approach for Examining Water Vapor and Deep
 1161 Convection Interactions in the Tropics. *Bull. Amer. Meteor. Soc.*, 96, 2151–2165, 2015.

1162 Antuña, J. C. and Barja, B.: Cirrus cloud optical properties measured with lidar in Camagüey, Cuba, *Óptica Pura y Aplicada*, 39, 11–16, 2006.

1163 Arraut, J.M., Nobre, C.A., Barbosa, H.M.J., Marengo J.A., and Obregon, G.: Aerial Rivers and Lakes: looking at large scale moisture transport, its relation to Amazonia and
 1164 to Subtropical Rainfall in South America, *J. Climate*, 25, pp. 543-556, doi: 10.1175/2011JCLI4189.1, 2012.

1165 Baars, H., Ansmann, A., Althausen, D., Engelmann, R., Heese, B., Müller, D., Artaxo, P., Paixao, M., Pauliquevis, T., and Souza, R.: Aerosol profiling with lidar in the
 1166 Amazon Basin during the wet and dry season, *J. Geophys. Res.*, 117, D21201, 2012.doi:10.1029/2012JD018338, 2012.

1167 Barja, B., Aroche, R.: Cirrus clouds at Camagüey, Cuba, *Proceedings of the SPARC 2000*, 2001.

1168 Barja, B. and Antuña, J. C.: The effect of optically thin cirrus clouds on solar radiation in Camagüey, Cuba, *Atmos. Chem. Phys.*, 11, 8625–8634, doi:10.5194/acp-11-8625-
 1169 2011, 2011.

1170 Barbosa, H. M. J., Barja, B., Pauliquevis, T., Gouveia, D. A., Artaxo, P., Cirino, G. G., Santos, R. M. N., and Oliveira, A. B.: A permanent Raman lidar station in the
 1171 Amazon: description, characterization, and first results, *Atmos. Meas. Tech.*, 7, 1745-1762, doi:10.5194/amt-7-1745-2014, 2014.

1172 Boucher, O., Randall, D., Artaxo, P., Bretherton, C., Feingold, G., Forster, P., Kerminen, V.-M., Kondo, Y., Liao, H., Lohmann, U., Rasch, P., Satheesh, S.K., Sherwood, S.,
 1173 Stevens, B., and Zhang, X.Y.: Clouds and Aerosols. In: *Climate Change 2013: The Physical Science Basis. Contribution of Working Group I to the Fifth Assessment
 1174 Report of the Intergovernmental Panel on Climate Change* [Stocker, T.F., D. Qin, G.-K. Plattner, M. Tignor, S.K. Allen, J. Boschung, A. Nauels, Y. Xia, V. Bex and
 1175 P.M. Midgley (eds.)]. Cambridge University Press, Cambridge, United Kingdom and New York, NY, USA, 2013.

1176 Bucholtz, A.: Rayleigh-scattering calculations for the terrestrial atmosphere, *Applied Optics* 34, 2765–2773, 1995.

1177 Burleyson, C., Z. Feng, S. Hagos, J. Fast, L. Machado, and S. Martin, *Spatial Variability of the Background Diurnal Cycle of Deep Convection around the GoAmazon2014/5
 1178 Field Campaign Sites. J. Appl. Meteor. Climatol.*, 55, 1579–1598, doi: 10.1175/JAMC-D-15-0229.1, 2016

Henrique de Melo J..., 1/10/2017 5:14 PM

Deleted: Pauliquevis, T., Adams, D. Artaxo, P., Cirino, G., Barja, B., Correia, A., Gomes, H., Gouveia, D. A., Padua, M. B., Rosario, N. M. E., Souza, R. Santos, R. M. Sapucci, L., and Portela, B. T.: ACONVEX—Aerosols, Clouds, cONvection, Experiment—A new site in central Amazonia for long term monitoring of aerosol-clouds-convection interactions. In: *AMS 95th Annual Meeting Proceedings* – Phoenix, Arizona, January 2015, 2015. ... [45]

1190 | Campbell, J. R., Vaughan, M. A., Oo, M., Holz, R. E., Lewis, J. R., and Welton, E. J., [Distinguishing cirrus cloud presence in autonomous lidar measurements](#), *Atmos. Meas. Tech.*, 8, 435-449, doi:10.5194/amt-8-435-2015, 2015.

1191 | Campbell, J., S. Lolli, J. Lewis, Y. Gu, and E. Welton, [Daytime Cirrus Cloud Top-of-the-Atmosphere Radiative Forcing Properties at a Midlatitude Site and Their Global Consequences](#). *J. Appl. Meteor. Climatol.*, 55, 1667–1679, doi: 10.1175/JAMC-D-15-0217.1, 2016

1192 | Cadet, B., Goldfarb, L., Fadulhe, D., Baldy, S., Giraud, V., Keckhut, P., and Réchou, A., A sub-tropical cirrus clouds climatology from Reunion Island (21°S, 55°E) lidar data set, *Geophys. Res. Lett.*, 30(3), 1130, doi:10.1029/2002GL016342, 2003.

1193 | Chen, W.; Chiang, C.; Nee, J.: Lidar ratio and depolarization ratio for cirrus clouds. *Applied Optics*, v. 41, n. 30, p. 6470 6476, 2002.

1194 | Chew B, Campbell J, Reid J, Giles D, Welton E, Salinas S, Liew S.: Tropical cirrus cloud contamination in sun photometer data. *Atmospheric Environment*;45 (37):6724-6731, 2011.

1195 | Comstock, J. M., Ackerman, T. P., and Mace, G. G.: Ground-based lidar and radar remote sensing of tropical cirrus clouds at Nauru Island: Cloud Statistics and radiative impacts, *J. Geophys. Res.*, 107, 4714, doi:10.1029/2002JD002203, 2002.

1196 | Fernald, F. G., Herman, B. M. and Reagan, J. A.: Determination of aerosol height distribution by lidar, *Appl. Opt.*, 11, 482–489, 1972.

1197 | Fortuin, J. P. F., Becker, C. R., Fujiwara, M., Immler, F., H. M. Kelder, Scheele, M. P., and Schrems, O., Verver, G. H. L.: Origin and transport of tropical cirrus clouds observed over Paramaribo, Suriname (5.8°N, 55.2°W), *J. Geophys. Res.*, 112, D09107, doi:10.1029/2005JD006420, 2007.

1198 | Giannakaki, E., Balis, D. S., Amiridis, V., and Kazadzis, S.: Optical and geometrical characteristics of cirrus clouds over a Southern European lidar station, *Atmos. Chem. Phys.*, 7, 5519–5530, doi:10.5194/acp-7-5519-2007, 2007.

1199 | Goldfarb, L., Keckhut, P., Chanin, M.-L., and Hauchecorne, A.: Cirrus climatological results from lidar measurements at OHP (44° N, 6° E), *Geophys. Res. Lett.*, 28, 1687–1690, 2001.

1200 | Hoareau, C., Keckhut, P., Noel, V., Chepfer, H., and Baray, J.-L.: A decadal cirrus clouds climatology from ground-based and spaceborne lidars above the south of France (43.9° N–5.7° E), *Atmos. Chem. Phys.*, 13, 6951–6963, doi:10.5194/acp-13-6951-2013, 2013.

1201 | Hogan, R. J., and Kew, S. F.: A 3D stochastic cloud model for investigating the radiative properties of inhomogeneous cirrus clouds. *Q. J. R. Meteorol. Soc.*, 131, 2585-2608, 2005.

1202 | Hong, G., Heygster, G., Miao, J., and Kunzi, K.: Detection of tropical deep convective clouds from AMSU-B water vapor channels measurements, *J. Geophys. Res.*, 110, D05205, doi:10.1029/2004JD004949, 2005.

1203 | Huffman, G.J., Adler, R.F., Bolvin, D.T., Gu, G., Nelkin, E.J., Bowman, K.P., Hong, Y., Stocker, E.F., and Wolff, D.B.,: The TRMM multi-satellite precipitation analysis: quasi-global, multi-year, combined-sensor precipitation estimates at fine scale. *J. Hydrometeorol.* 8 (1), 38–55, 2007.

1204 | Immler, F. and Schrems, O.: LIDAR measurements of cirrus clouds in the northern and southern midlatitudes during INCA (55° N, 53° S): A comparative study, *Geophys. Res. Lett.*, 29, 1809, doi:10.1029/2002GL015076, 2002a.

Henrique de Melo J..., 1/10/2017 5:14 PM

Deleted: Dupont, J.-Haefelin, M., Morille, Y., Noël, V., Keckhut, P., Winker, D., Comstock, J., Chervet, P., and Robin, A.: Macrophysical and optical properties of midlatitude cirrus clouds from four ground-based lidars and collocated CALIOP observations, *J. 115*, D00H24, doi:10.1029/2009JD011943, 2010. +
Fitzjarrald, D. Sakai, R. Moraes, O. L. L., de L., de Oliveira, R. Acevedo, O. C., Czikowsky, Mand Beldini, T.: Spatial and temporal rainfall variability near the Amazon-Tapajós confluence. *J.*, 113, G00B11, doi:10.1029/2007JG000596, 2008. +

Henrique de Melo J..., 1/10/2017 5:14 PM

Deleted: Fitzjarrald, D. Sakai, R. Moraes, O. L. L., de Oliveira, R. Acevedo, O. C., Czikowsky, Mand Beldini, T.: Spatial and temporal rainfall variability near the Amazon-Tapajós confluence. *J.*, 113, G00B11, doi:10.1029/2007JG000596, 2008. +

1237 Immler, F., and Schrems, O.: Determination of tropical cirrus properties by simultaneous LIDAR and radiosonde measurements, *Geophys. Res. Lett.*, 29/23, 4,
 1238 doi:10.1029/2002GL015076, 2002b.

1239 | [International meteorological vocabulary. WMO, No. 182. TP. 91. Geneva \(Secretariat of the World Meteorological Organization\) 1966. Pp. xvi, 276. Sw. fr. 40. Q.J.R. Meteorol. Soc., 93: 148. doi:10.1002/qj.49709339524](#)

1240 | Jensen, E. J., Toon, O. B., Selkirk, H. B., Spinhirne, J. D., and Schoeberl, M. R.: On the formation and persistence of subvisible cirrus clouds near the tropical tropopause, *J. Geophys. Res.*, 101(D16), 21361–21375, doi:10.1029/95JD03575, 1996.

1241 | Khvorostyanov, V. I., and Sassen, K.: Microphysical processes in cirrus and their impact on radiation A Mesoscale Modeling Perspective, in *Cirrus* ed D Lynch, K Sassen, D O C Starr and G Stephens (Oxford: Oxford University Press) pp 397–432, 2002.

1242 | Kienast-Sjögren, E., Rolf, C., Seifert, P., Krieger, U. K., Luo, B. P., Krämer, M., and Peter, T., [Climatological and radiative properties of midlatitude cirrus cloud derived by automatic evaluation of lidar measurements, Atmos. Chem. Phys., 16, 7605-7621, doi:10.5194/acp-16-7605-2016, 2016.](#)

1243 | Kim, Y., Kim, S.-W., Kim, M.-H. and Yoon, S.-C.: Geometric and optical properties of cirrus clouds inferred from three-year ground-based lidar and CALIOP measurements over Seoul, Korea, *Atmospheric Research*, 139, 27–35, 2014.

1244 | Klett, J.D.: Stable analytical inversion solution for processing lidar returns. *Appl. Opt.* 20(2), 211–220, 1981.

1245 | Krämer, M., Rolf, C., Luebke, A., Afchine, A., Spelten, N., Costa, A., Meyer, J., Zöger, M., Smith, J., Herman, R. L., Buchholz, B., Ebert, V., Baumgardner, D., Borrmann, S., Klingebiel, M., and Avallone, L.: [A microphysics guide to cirrus clouds – Part 1: Cirrus types, Atmos. Chem. Phys., 16, 3463-3483, doi:10.5194/acp-16-3463-2016, 2016a.](#)

1246 | Martina Krämer, Armin Afchine, Linnea Avallone, Darrel Baumgardner, Stephan Borrmann, Bernhard Buchholz, Anja Costa, Volker Ebert, David Fahey, Robert Herman, Eric Jensen, Marcus Klingebiel, P. Lawson S. Woods, Anna Luebke, Jessica Meyer, Christian Rolf, A. Rollins, T. Thornberry, Jessica Smith, Nicole Spelten, Martin Zöger, [Microphysical properties of cirrus clouds between 75N and 25S derived from extensive airborne in-situ observations, In.: XVII International Conference on Clouds & Precipitation, Manchester, 25-29 July, 2016b.](#)

1247 | Lakkis, G.S., Lavorato, M., and Canziani, O.P.: Monitoring cirrus clouds with lidar in the Southern Hemisphere: a local study over Buenos Aires. 1. Tropopause heights. *Atmos. Res.* 92 (1), 18–26, 2009.

1248 | Lin, L., Fu, Q., Zhang, H., Su, J., Yang, Q., and Sun, Z.: Upward mass fluxes in tropical upper troposphere and lower stratosphere derived from radiative transfer calculations, *J. Quant. Spectrosc. Radiat. Transfer*, 117, 114–122, 2013.

1249 | Liou, K. N.: Influence of cirrus clouds on weather and climate processes: A global perspective. *Mon. Wea. Rev.*, 114, 1167–1199, 1986.

1250 | Liu, C., and Zipser, E. J., [Global distribution of convection penetrating the tropical tropopause, J. Geophys. Res., 110, D23104, doi:10.1029/2005JD006063, 2005](#)

1251 | Liu, C., and Zipser, E. J.: Implications of the day versus night differences of water vapor, carbon monoxide, and thin cloud observations near the tropical tropopause, *J. Geophys. Res.*, 114, D09303, doi:10.1029/2008JD011524, 2009.

Henrique de Melo J.... 1/10/2017 5:14 PM
Deleted: Jiang, J. H., Su, H., Zhai, Ch., Shen, T. J., Wu, T., Zhang, J., Cole, J. N. von Salzen, K., Donner, L.Seman, Ch., Del Genio, A., Nazarenko, L. S., Dufresne, J.-L., Watanabe, M., Morcrette, C., Koshiro, T., Kawai, H., Gettelman, A., Millán, L., Read, W.G., Livesey, N. J., Kasai, Y., and Shiotani, M.: Evaluating the Diurnal Cycle of Upper-Tropospheric Ice Clouds in Climate Models Using SMILES Observations. 72, 1022–1044. doi:10.1175/JAS-D-14-0124.1, 201 ... [46]

1276 Lynch, D. K., Sassen, K., Starr, D. O., and Stephens, G.: *Cirrus*. Oxford University Press, 480 pp., 2002.

1277 | [Mace, G. G., R. Marchand, Q. Zhang, and G. Stephens, Global hydrometeor occurrence as observed by CloudSat: Initial observations from summer 2006](#), *Geophys. Res. Lett.*, 34, L09808, doi:10.1029/2006GL029017, 2007.

1278 | Machado, L.A.T., Laurent, H., and Lima, A.A.: Diurnal march of the convection observed during TRMM-WETAMC/LBA, *J. Geophys. Res.*, 107(D20), 8064, doi:10.1029/2001JD000338, 2002.

1281 | Machado, L.A.T.; Laurent, H.; Dessay, N.; Miranda, I.: Seasonal and diurnal variability of convection over the Amazonia - A comparison of different vegetation types and large scale forcing. *Theoretical and Applied Climatology*, 78, 61-77, doi: 10.1007/s00704-004-0044-9. 2004.

1283 | Machado, L.A.T., Silva Dias, M.A.F., Morales, C., Fisch, G., Vila,D., Albrecht, R., Goodman, S.J., Calheiros, A.J.P., Biscaro, T., Kummerow, C., Cohen, J., Fitzjarrald, D., Nascimento, E.L., Sakamoto, M.S., Cunningham, C., Chaboureau, J.-P., Petersen, W.A., Adams, D.K., Baldini, L., Angelis, C.F., Sapucci, L.F., Salio, P., Barbosa, H.M.J., Landulfo, E., Souza, R.A.F., Blakeslee, R.J., Bailey, J., Freitas, S., Lima, W.F.A., Tokay, A.: THE CHUVA PROJECT: how does convection vary across Brazil? *Bull. Am. Meteor. Soc.*, 1365–1380, doi:10.1175/BAMS-d-13-00084.1, 2014.

1287 | Martin, S. T., Artaxo, P., Machado, L. A. T., Manzi, A. O., Souza, R. A. F., Schumacher, C., Wang, J., Andreae, M. O., Barbosa, H. M. J., Fan, J., Fisch, G., Goldstein, A. H., Guenther, A., Jimenez, J. L., Pöschl, U., Silva Dias, M. A., Smith, J. N., and Wendisch, M.: Introduction: Observations and Modeling of the Green Ocean Amazon (GoAmazon2014/5), *Atmos. Chem. Phys.*, 16, 4785-4797, doi:10.5194/acp-16-4785-2016, 2016.

1290 | [McCalla, C., 1981: Objective Determination of the Tropopause Using WMO Operational Definitions](#), Office Note 246, U.S. Department of Commerce, NOAA, NWS, NMC, 18pp, October 1981.

1292 | Nazaryan, H., McCormick, M. P., and Menzel, W. P.: Global characterization of cirrus clouds using CALIPSO data, *J. Geophys. Res.*, 113, D16211, doi:10.1029/2007JD009481, 2008.

1294 | Pace, G., Cacciani, M., di Sarra, A., Fiocco, G., and Fuà, D.: Lidar observations of equatorial cirrus clouds at Mahé Seychelles, *J. Geophys. Res.*, 108(D8), 4236, doi:10.1029/2002JD002710, 2003.

1296 | Pandit, A. K., Gadhavi, H. S., Venkat Ratnam, M., Raghunath, K., Rao, S. V. B., and Jayaraman, A.; Long-term trend analysis and climatology of tropical cirrus clouds using 16 years of lidar data set over Southern India. *Atmos. Chem. Phys.*, 15, 13833–13848, doi:10.5194/acp-15-13833-2015, 2015

1298 | [Platt, C. M. R., Remote sounding of high clouds. III: Monte Carlo calculations of multiple scattered lidar returns](#), *J. Atmos. Sci.*, 38, 156–167, 1981

1299 | Randel, W. J. and Jensen, E. J.: Physical processes in the tropical tropopause layer and their roles in a changing climate, *Nat. Geosci.*, 6, 169–176, doi:10.1038/ngeo1733, 2013.

1301 | Sasano Y., and Nakane H.: Significance of the extinction/backscatter ratio and the boundary value term in the solution for the two-component lidar equation”, *Appl. Opt.*, vol. 23, 11–13, 1984.

1303 | Sassen, K., and B. S. Cho, B. S., [Subvisual/thin cirrus dataset for satellite verification and climatological research](#), *J. Appl. Meteorol.*, 31, 1275–1285, 1992

Henrique de Melo J..., 1/10/2017 5:14 PM

Deleted: Quante, M., and Starr, D. O'C.:
Dynamical processes in cirrus clouds: Review of observational results. Chapter 17 in: D. Lynch, K. Sassen, D.O'C. Starr, G. Stephens (eds.): *Cirrus*. Oxford University Press, New York, 346-374, 2002. [...](#)

1310 | [Sassen](#), K., Starr, D. O'C., and Uttal, T.: Mesoscale and Microscale Structure of Cirrus Clouds: Three Case Studies, *J of the Atmos. Sci.* 46:3, 371-396, 1989.

1311 | Sassen, K. and Campbell, J. R.: A midlatitude cirrus cloud climatology from the facility for atmospheric remote sensing. Part I: Macrophysical and synoptic properties, *J. Atmos. Sci.*, 58, 481-496, 2001.

1312 | Sassen, K.: Cirrus Clouds. A Modern Perspective, In Cirrus D. Lynch, K. Sassen, D. O'C Starr, and G. Stephens Eds., Oxford University Press, 136-146, 2002.

1313 | Sassen, K., Wang, Z., and Liu, D.: Global distribution of cirrus clouds from CloudSat/Cloud-Aerosol Lidar and Infrared Pathfinder Satellite Observations (CALIPSO) measurements, *J. Geophys. Res.*, 113, D00A12, doi:10.1029/2008JD009972, 2008.

1314 | Sassen, K., Wang, Z., and Liu, D.: Cirrus clouds and deep convection in the tropics: Insights from CALIPSO and CloudSat, *J. Geophys. Res.*, 114, D00H06, 1315 | doi:10.1029/2009JD011916, 2009.

1316 | Seifert, P.; Ansmann, A.; Muâller, D.; Wandinger, U.; Althausen, D.; Heymsfield, A. J.; Massie, S. T.; Schmitt, C.: Cirrus optical properties observed with lidar, radiosonde 1317 | and satellite over the tropical indian ocean during the aerosol-polluted northeast and clean maritime southwest monsoon. *J. Geophys. Res.*, v. 112, p. D17205, 2007.

1318 | Silva, V. B. S., Kousky, V. E., and Higgins, R. W.: Daily Precipitation Statistics for South America: An Intercomparison between NCEP Reanalyses and Observations. *J. 1319 | Hydrometeorol.*, 12, 101-117. DOI: 10.1175/2010JHM1303.1, 2011.

1320 | [Stein, A.F.](#), [Draxler, R.R.](#), [Rolph, G.D.](#), [Stunder, B.J.B.](#), [Cohen, M.D.](#), and [Ngan, F.](#), NOAA's HYSPLIT atmospheric transport and dispersion modeling system, *Bull. Amer. 1321 | Meteor. Soc.*, 96, 2059-2077, doi:10.1175/BAMS-D-14-00110.1, 2015

1322 | Stubenrauch, C. J., Chédin, A., Rädel, G., Scott, N. A., and Serrar, S.: Cloud Properties and Their Seasonal and Diurnal Variability from TOVS Path-B. *J. Climate*, 19, 5531- 1323 | 5553, 2006.

1324 | Tanaka, L. M. d. S., Satyamurty, P., and Machado, L. A. T.: Diurnal variation of precipitation in central Amazon Basin. *Int. J. Climatol.* 34, 3574-3584, DOI: 1325 | 10.1002/joc.3929, 2014.

1326 | Thorsen, T. J., Qiang, F., and Comstock, J. M.: Comparison of the CALIPSO satellite and ground-based observations of cirrus clouds at the ARM TWP sites, *J. Geophys. 1327 | Res.*, 116, D21203, doi:10.1029/2011JD015970, 2011.

1328 | [Thorsen, T.](#) and [Q. Fu](#), Automated Retrieval of Cloud and Aerosol Properties from the ARM Raman Lidar. Part II: Extinction. *J. Atmos. Oceanic Technol.*, 32, 1999-2023, 1329 | doi: 10.1175/JTECH-D-14-00178.1, 2015.

1330 | [Wandinger, U.](#), Multiple-scattering influence on extinction- and backscatter-coefficient measurements with Raman and high-spectral-resolution lidars, *Appl. Optics*, 37, 417- 1331 | 427, 1998.

1332 | Wang, T., and Dessler, A. E.: Analysis of cirrus in the tropical tropopause layer from CALIPSO and MLS data: A water perspective, *J. Geophys. Res.*, 117, D04211, 1333 | doi:10.1029/2011JD016442, 2012.

1334 | Wendisch, M., et al.: The ACRIDICON-CHUVA campaign: Studying tropical deep convective clouds and precipitation over Amazonia using the new German research 1335 | aircraft HALO. *Bull. Am. Met. Soc.*, accepted, doi:10.1175/BAMS-D-14-00255.1, 2016

Henrique de Melo J..., 1/10/2017 5:14 PM

Deleted: Starr, D. O'C., and Quante, M.:
Dynamical processes in cirrus clouds: Concepts and models. Chapter 18 in: D. Lynch, K. Sassen, D.O'C. Starr, G. Stephens (eds.): Cirrus. Oxford University Press, New York, 375-396, 2002. *

1343 | Westbrook, C. D., Illingworth, A. J., O'Connor, E. J. and Hogan, R. J., Doppler lidar measurements of oriented planar ice crystals falling from supercooled and glaciated layer

1344 | clouds. *Q.J.R. Meteorol. Soc.*, 136: 260–276, 2010.

1345 | Wylie, D. P., Jackson, D. L., Menzel, W. P., and Bates, J. J.: Trends in global cloud cover in two decades of HIRS observations. *J. Climate*, 18, 3021–3031, 2005.

1346 | Yang, P., Hong, G., Dessler, A. E., Ou, S. C., Liou, K. N., Minnis, P., and Hashvardhan,: Contrails and induced cirrus: Optics and radiation. *Bull. Amer. Meteor. Soc.*, 91,

1347 | 473–478, 2010a.

1348 | Yang, Q., Fu, Q., and Hu, Y.: Radiative impacts of clouds in the tropical tropopause layer, *J. Geophys. Res.*, 115, D00H12, doi:10.1029/2009JD012393, 2010b.

1349 | Young, S.: Analysis of lidar backscatter profiles in optically thin cirrus, *Appl. Opt.*, 34, 7019–7031, 1995.

1350 |

Henrique de Melo J..., 1/10/2017 5:14 PM

Deleted: Zerefos, C. S., Eleftheratos, K., Balis, D. S., Zanis, P., Tselioudis, G., and Meleti, C.: Evidence of impact of aviation on cirrus cloud formation, *Atmos.* 3, 1633–1644, doi:10.5194/acp-3-1633-2003, 2003. -

Tables:

Table 1. Summary of some recent cirrus [cloud](#) studies based on at least a few months of ground-based lidar observations in the tropics and mid-latitudes. The first columns show the period of study and laser wavelength (nm) for each site location, for which more than one study might be available. The cirrus characteristics are those reported by the different authors, which might include: base and top height (km), thickness (km), base and top temperature (°C), frequency of occurrence (%) and lidar-ratio (sr).

Measurement site	Location	Period of study	Wavelength [nm]	Average values									
				Height [km]			Temp. [°C]		Frequency [%]		LR[sr]		
				Base	Top	Thick.	Base	Top	SVC	Thin			
Salt Lake City, Utah, USA	40.8°N 111.8°W	1986 to 1996	694	8.8	11.2	1.8	-34.4	-53.9	50	-		Sassen and Campbell (2001)	
Haute Provence, France	43.9°N 5.7°E	1997 to 2007	532/10 64	9.3	10.7	1.4			38		18.2	Goldfarb et al. (2001) Hoareau et al. (2013)	
Thessaloniki, Greece	40.6°N 22.9°E	2000 to 2006	355/53 2	8.6	11.7	2.7	-38	-65		57	30	Giannakaki et al. (2007)	
Seoul, South Korea	37°N, 127°E	2006 to 2009	532/10 64	8.8	10.6						20	Kim et al. (2009)	
Buenos Aires, Argentina	34.6 °S, 58.5 °W	2001 to 2005	532	9.6	11.8	2.4		-64.5				Lakkis et al.(2008)	
Reunion Island	21°S, 55°E	1996 to 2001	532	11	14				65		18.3	Cadet et al. (2003)	
Camagüey, Cuba	21.4° N, 77.9° W	1993 to 1998	532	11.6	13.8				25		10	Antuña and Barja, (2006)	
Gadanki, India	13.5 N, 79.2 E	1998 to 2013	532	13.0	15.3	2.3		-65	52	36	25	Pandit et al., (2015)	
Hulule, Maldives	4.1°N, 73.3°E	1999, 2000	532	11.9	13.7	1.8	-50	-65	15	49	32	Seifert et al. (2007)	
Mahé, Seychelles	4.4 °S, 55.3 °E	Feb-Mar 1999	532			0.2-2.0					19	Pace et al., (2003)	
Nauru Island	0.5 °S, 166.9 °E	Apr-Nov 1999	532	~14	~16							Comstock et al. (2002)	

Henrique de Melo J..., 1/10/2017 5:14 PM

Deleted: clouds

Henrique de Melo J..., 1/10/2017 5:14 PM

Deleted: Campbel

Henrique de Melo J..., 1/10/2017 5:14 PM

Deleted: Prov.,

Henrique de Melo J..., 1/10/2017 5:14 PM

Deleted: .

Henrique de Melo J..., 1/10/2017 5:14 PM

Deleted: Mahe',

Henrique de Melo J..., 1/10/2017 5:14 PM

Deleted: -

Henrique de Melo J..., 1/10/2017 5:14 PM

Deleted: -

Table 2. Summary of column-integrated statistics for the total time of observation, as well as for the wet, transition and dry seasons. Frequency of occurrence is calculated using a conditional sampling to avoid biases (section 2.4). Mean cirrus cloud properties and standard deviation of the sample (in parenthesis) are shown. The standard deviations of the mean can be calculated and used to determine if seasonal differences (wet-dry) of the mean values are statistically significant to the 95% confidence level (indicated as *). Geometrical properties are not given because most cloud profiles have more than one layer of cirrus. Lidar ratio is calculated as a column average.

	<u>Total</u>	<u>Wet</u>	<u>Transition</u>	<u>Dry</u>
<u>Observation time [%]</u> ^a	<u>37.4</u>	<u>41.5</u>	<u>21.9</u>	<u>48.9</u>
<u>N. prof. measured</u> ^b	<u>36844</u>	<u>13828</u>	<u>7423</u>	<u>15593</u>
<u>N. prof. used in analysis</u> ^c	<u>16025</u>	<u>3458</u>	<u>2099</u>	<u>10468</u>
<u>N. prof. discarded for apparent top</u> ^d	<u>476</u>	<u>223</u>	<u>148</u>	<u>105</u>
<u>Frequency of Occurrence [%]*</u>	<u>73.8</u>	<u>88.1</u>	<u>74.2</u>	<u>59.2</u>
<u>N. prof. w/ cirrus</u>	<u>11252</u>	<u>3145</u>	<u>1706</u>	<u>6397</u>
<u>Frequency of Occurrence, Opaque [%]*</u>	<u>22.6</u>	<u>31.3</u>	<u>24.6</u>	<u>11.8</u>
<u>N. prof. w/ cirrus, Opaque</u>	<u>3327</u>	<u>1316</u>	<u>610</u>	<u>1401</u>
<u>Frequency of Occurrence, Thin [%]*</u>	<u>32.8</u>	<u>37.9</u>	<u>36.5</u>	<u>23.9</u>
<u>N. prof. w/ cirrus, Thin</u>	<u>4577</u>	<u>1224</u>	<u>798</u>	<u>2555</u>
<u>Frequency of Occurrence, SVC [%]*</u>	<u>18.3</u>	<u>18.7</u>	<u>13.0</u>	<u>23.3</u>
<u>N. prof. w/ cirrus, SVC</u>	<u>3322</u>	<u>603</u>	<u>296</u>	<u>2423</u>
<u>Cloud Optical Depth*</u>	<u>0.35 (0.55)</u>	<u>0.47 (0.65)</u>	<u>0.40 (0.57)</u>	<u>0.25 (0.45)</u>
<u>Max Backscatter Altitude [km]*</u>	<u>13.4 (2.0)</u>	<u>13.4 (2.2)</u>	<u>13.3 (2.2)</u>	<u>13.6 (1.7)</u>
<u>Temperature Max. Back. Alt. [°C]*</u>	<u>-60 (15)</u>	<u>-60 (16)</u>	<u>-59 (17)</u>	<u>-62 (13)</u>
<u>Lidar Ratio [sr]*</u> ^e	<u>23.6 (8.1)</u>	<u>22.8 (8.0)</u>	<u>22.8 (7.8)</u>	<u>24.6 (7.7)</u>
<u>Num. of cirrus layers per cloud prof.</u>	<u>1.41 (0.63)</u>	<u>1.62 (0.77)</u>	<u>1.61 (0.67)</u>	<u>1.25 (0.48)</u>

^a Fraction of observation time to total possible time (21h per day)

^b Total number of profiles measured, i.e. not screened for low clouds or precipitation

^c Refers to the number of 5-min profiles with high enough SNR (section 2.4)

^d Number of profiles with apparent cirrus top, considering only good profiles

^e All layers in the same profile share the same average LR

Table 3. Summary of layer-statistics for the total time of observation, as well as for the wet, transition and dry seasons. Mean cirrus cloud properties and standard deviation of the sample (in parenthesis) are shown. The standard deviations of the mean can be calculated and used to determine if seasonal differences (wet-dry) are statistically significant to the 95% confidence level (indicated as *). Lidar ratio is calculated as a column average.

	<u>Total</u>	<u>Wet</u>	<u>Transition</u>	<u>Dry</u>
<u>All Layers</u>				
<u>Num. of cirrus layers</u>	<u>15824</u>	<u>5096</u>	<u>2739</u>	<u>7989</u>
<u>Base Altitude [km]*</u>	<u>12.9 (2.2)</u>	<u>12.8 (2.4)</u>	<u>12.6 (2.3)</u>	<u>13.0 (1.9)</u>
<u>Top Altitude [km]</u>	<u>14.3 (1.9)</u>	<u>14.3 (2.0)</u>	<u>14.1 (2.0)</u>	<u>14.3 (1.6)</u>
<u>Thickness [km]*</u>	<u>1.4 (1.1)</u>	<u>1.5 (1.2)</u>	<u>1.5 (1.1)</u>	<u>1.3 (1.0)</u>
<u>Cloud Optical Depth*</u>	<u>0.25 (0.46)</u>	<u>0.30 (0.52)</u>	<u>0.26 (0.47)</u>	<u>0.20 (0.40)</u>
<u>Max Backscatter Altitude [km]</u>	<u>13.6 (2.0)</u>	<u>13.7 (2.3)</u>	<u>13.5 (2.2)</u>	<u>13.6 (1.8)</u>
<u>Lidar Ratio [sr]*</u>	<u>23.3 (8.0)</u>	<u>22.6 (8.1)</u>	<u>22.8 (7.9)</u>	<u>22.4 (7.9)</u>
<u>Relative freq. opaque cirrus [%]*</u>	<u>20.5</u>	<u>25.2</u>	<u>21.0</u>	<u>17.4</u>
<u>Relative freq. thin cirrus [%]</u>	<u>37.8</u>	<u>37.0</u>	<u>43.2</u>	<u>36.5</u>
<u>Relative freq. SVC [%]*</u>	<u>41.6</u>	<u>37.8</u>	<u>35.8</u>	<u>46.0</u>
<u>Base above the tropopause [%]*</u>	<u>5.9</u>	<u>6.9</u>	<u>5.5</u>	<u>5.3</u>
<u>Top above the tropopause [%]*</u>	<u>15.7</u>	<u>18.7</u>	<u>16.1</u>	<u>12.9</u>
<u>Opaque Layers</u>				
<u>Num. of opaque layers</u>	<u>3251</u>	<u>1283</u>	<u>574</u>	<u>1394</u>
<u>Base Altitude [km]*</u>	<u>10.7 (1.5)</u>	<u>10.6 (1.6)</u>	<u>10.4 (1.5)</u>	<u>10.8 (1.2)</u>
<u>Top Altitude [km]</u>	<u>13.4 (1.6)</u>	<u>13.5 (1.7)</u>	<u>13.1 (1.6)</u>	<u>13.6 (1.4)</u>
<u>Thickness [km]*</u>	<u>2.76 (1.02)</u>	<u>2.84 (1.07)</u>	<u>2.65 (1.04)</u>	<u>2.73 (0.94)</u>
<u>Cloud Optical Depth*</u>	<u>0.93 (0.64)</u>	<u>1.00 (0.66)</u>	<u>0.90 (0.66)</u>	<u>0.86 (0.59)</u>
<u>Max Backscatter Altitude [km]</u>	<u>12.0 (1.7)</u>	<u>12.1 (1.9)</u>	<u>11.6 (1.7)</u>	<u>12.1 (1.5)</u>
<u>Lidar Ratio [sr]*</u>	<u>25.7 (6.3)</u>	<u>26.0 (6.7)</u>	<u>25.8 (6.6)</u>	<u>25.3 (5.7)</u>
<u>Thin Layers</u>				
<u>Num. of thin layers</u>	<u>5985</u>	<u>1888</u>	<u>1183</u>	<u>2914</u>
<u>Base Altitude [km]*</u>	<u>12.9 (1.7)</u>	<u>13.1 (1.9)</u>	<u>12.9 (1.8)</u>	<u>12.8 (1.4)</u>
<u>Top Altitude [km]*</u>	<u>14.4 (1.7)</u>	<u>14.6 (2.0)</u>	<u>14.4 (1.8)</u>	<u>14.3 (1.4)</u>
<u>Thickness [km]*</u>	<u>1.46 (0.78)</u>	<u>1.42 (0.82)</u>	<u>1.49 (0.78)</u>	<u>1.47 (0.74)</u>
<u>Cloud Optical Depth</u>	<u>0.12 (0.07)</u>	<u>0.12 (0.07)</u>	<u>0.12 (0.07)</u>	<u>0.11 (0.07)</u>
<u>Max Backscatter Altitude [km]*</u>	<u>13.7 (1.7)</u>	<u>13.9 (1.9)</u>	<u>13.7 (1.9)</u>	<u>13.5 (1.5)</u>
<u>Lidar Ratio [sr]*</u>	<u>22.8 (7.9)</u>	<u>21.8 (7.7)</u>	<u>21.6 (7.4)</u>	<u>24.3 (8.1)</u>
<u>SVC Layers</u>				
<u>Num. of SVC layers</u>	<u>6581</u>	<u>1924</u>	<u>980</u>	<u>3677</u>
<u>Base Altitude [km]*</u>	<u>14.4 (1.9)</u>	<u>14.7 (2.1)</u>	<u>14.4 (2.1)</u>	<u>14.2 (1.6)</u>
<u>Top Altitude [km]*</u>	<u>14.9 (1.9)</u>	<u>15.2 (2.1)</u>	<u>15.0 (2.1)</u>	<u>14.7 (1.6)</u>
<u>Thickness [km]</u>	<u>0.51 (0.37)</u>	<u>0.50 (0.38)</u>	<u>0.53 (0.38)</u>	<u>0.51 (0.36)</u>
<u>Cloud Optical Depth</u>	<u>0.011 (0.008)</u>	<u>0.011 (0.008)</u>	<u>0.012 (0.009)</u>	<u>0.011 (0.008)</u>
<u>Max Backscatter Altitude [km]*</u>	<u>14.6 (1.9)</u>	<u>14.9 (2.1)</u>	<u>14.7 (2.1)</u>	<u>14.4 (1.6)</u>
<u>Lidar Ratio [sr]*</u>	<u>21.6 (8.4)</u>	<u>19.9 (7.6)</u>	<u>21.5 (8.1)</u>	<u>23.5 (9.0)</u>

Figures:

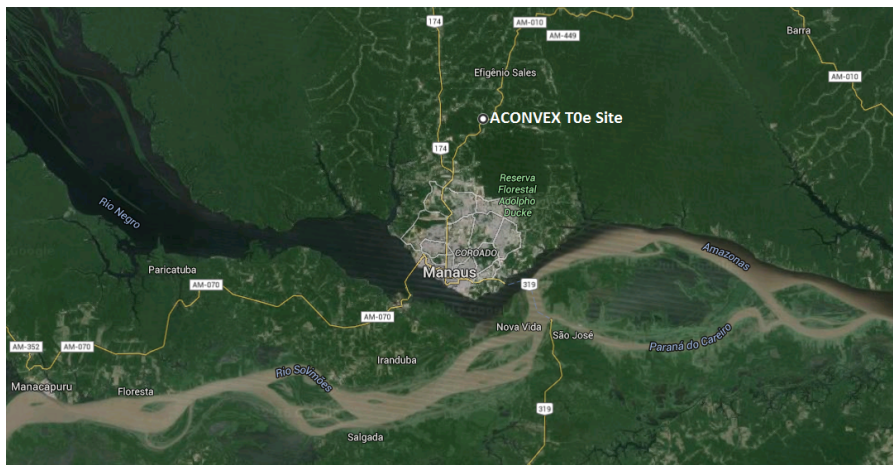


Figure 1. Satellite-based map (Google Earth) showing the location of the lidar site (ACONVEX T0e, 2.89°S 59.97°W), 30 km upwind (north) from downtown Manaus-AM, Brazil.

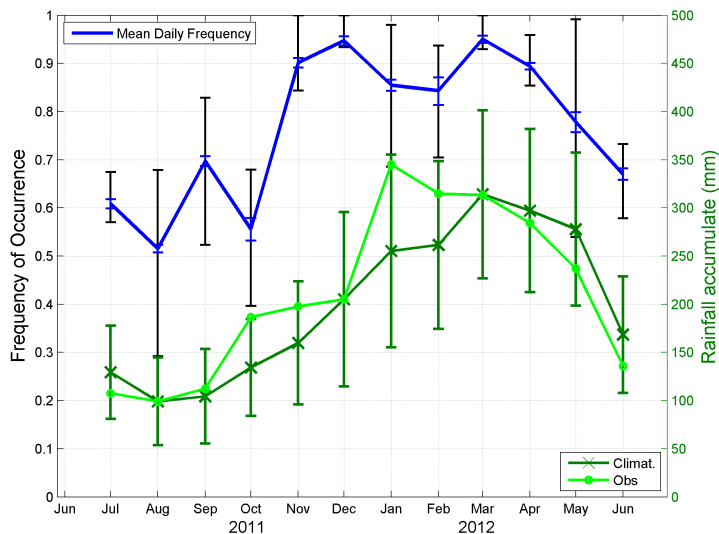


Figure 2. Monthly frequency of occurrence of cirrus clouds from July 2011 to June 2012 (blue line) with the associated statistical error (black). Accumulated (light green) and climatological (dark green) rainfall, shown on the right axis, were obtained from the TRMM 3B42 version 7 dataset averaged over an area of $10^\circ \times 10^\circ$.

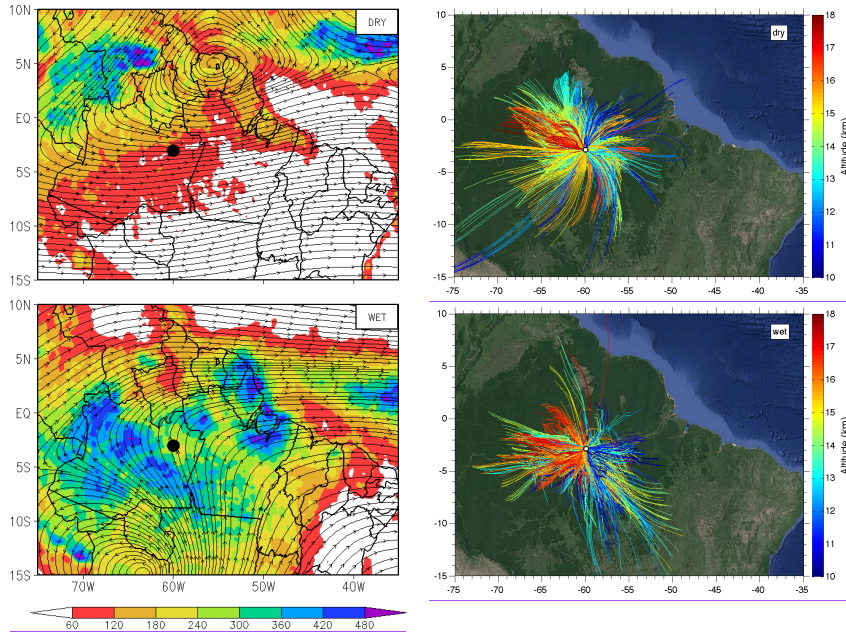


Figure 3. Left panels show mean precipitation (colors, mm month^{-1}) from the TRMM 3B42 version 7 and mean wind field (vectors, m/s) at 150 hPa ($\sim 14.3 \text{ km}$) from ECMWF ERA Interim reanalysis. Right panels show 24 h back trajectories of air masses arriving at the site at the time and altitude that cirrus layers were detected. Results are shown separately for the dry (JJAS, top) and wet months (JFMA, bottom). Backward trajectories were computed using HYSPLIT model with 0.5° resolution winds from GDAS/NOAA. The experimental site location is indicated in all panels with a circle.

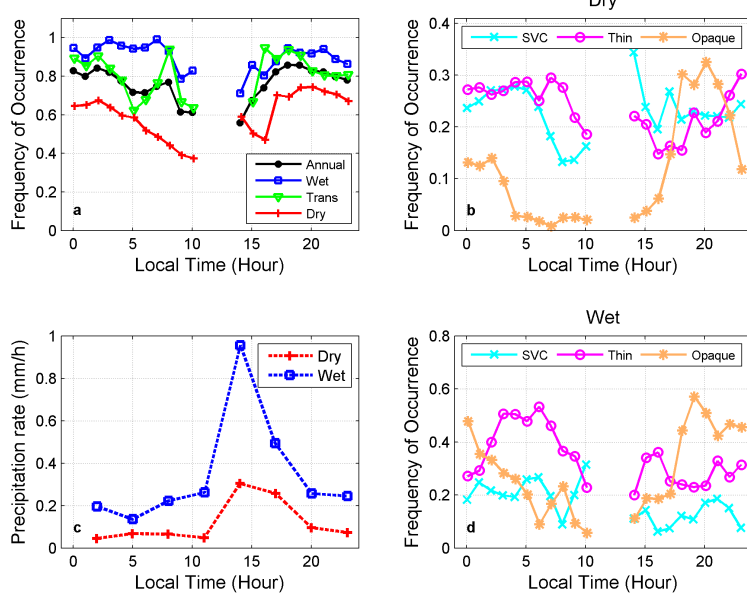


Figure 4. Panel (a) shows the daily cycles of the hourly frequency of occurrence of cirrus clouds for the annual, wet, transition and dry periods. The same is shown for SVC, thin and opaque cirrus clouds during the dry (b) and wet (d) seasons. Mean observed precipitation rate (mm/h) from TRMM version 7 over an area of $2^\circ \times 2^\circ$ centered on the site, for the dry and wet periods, is given in panel (c).

Unknown

Formatted: Font:(Default) Times New Roman, 10 pt

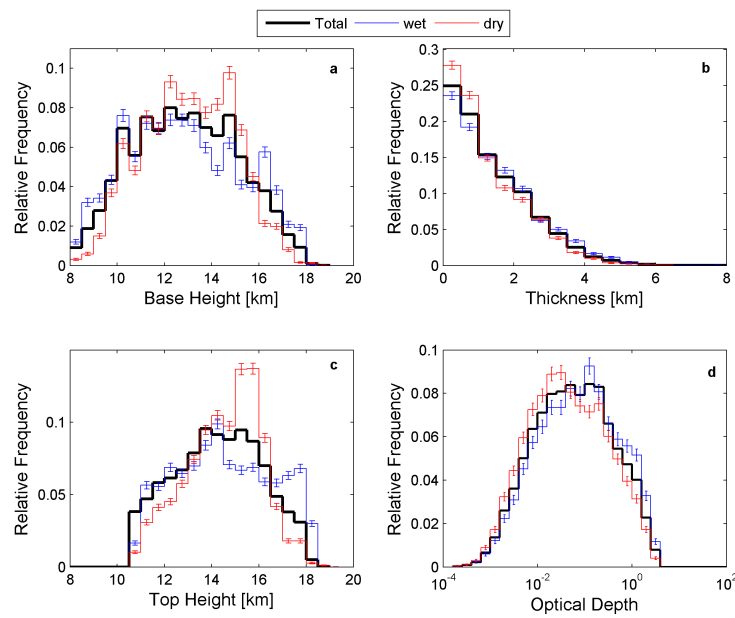


Figure 5. Panels show the normalized histograms of (a) cirrus cloud base, (b) cloud geometrical thickness, (c) cirrus cloud top, and (d) optical depth, for the overall period (black), wet season (JFMA, red) and dry season (JJAS, blue). Error bars indicate the counting statistics uncertainty.

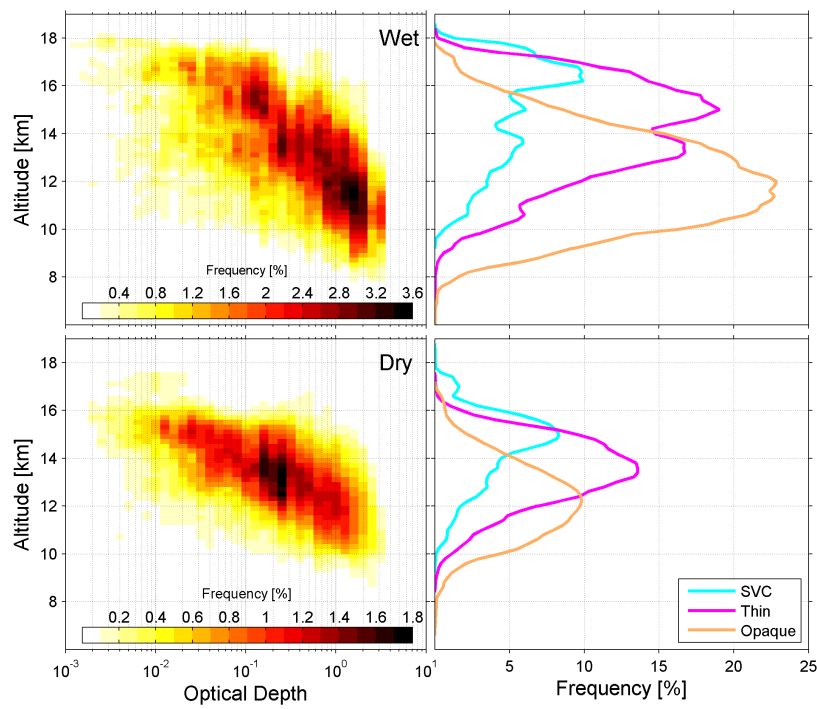


Figure 6. Two-dimensional histograms of cirrus frequency of occurrence with altitude as a function of optical depth during the wet (top) and dry (bottom) season months are shown on the left. The same is shown on the right but integrated for SVC, thin and opaque cirrus clouds optical depths.

Unknown
Formatted: Font:9 pt

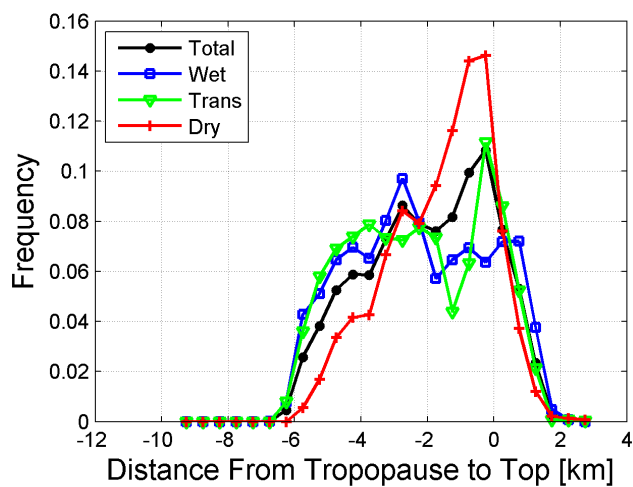
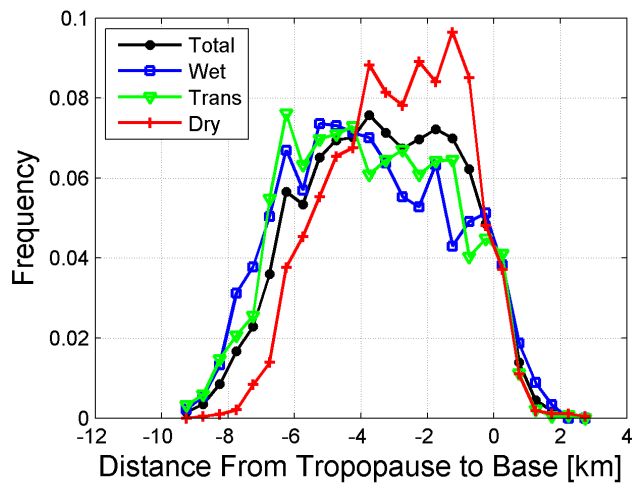
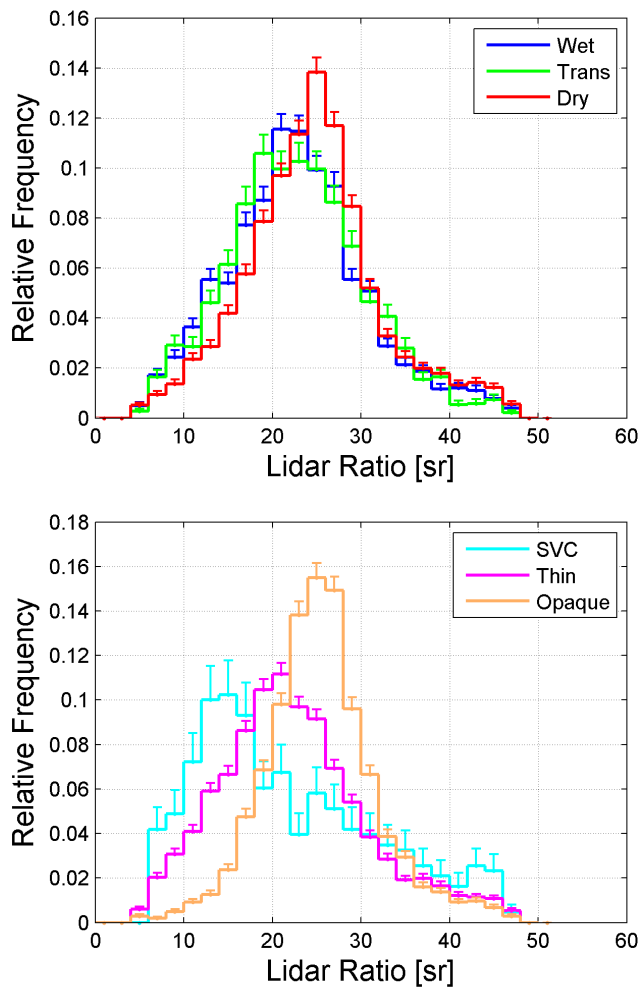


Figure 7. Normalized histograms of the distance of the tropopause to the cirrus base and top are shown for overall period (black) and each season (colors). Negative values mean that clouds are below tropopause. The average tropopause altitude was 16.2 ± 0.4 km.

Unknown

Formatted: Font:(Default) Times New Roman, 10 pt



Unknown

Formatted: Font:(Default) Times New Roman, 10 pt

Figure 8. Normalized histograms of the lidar ratio, already corrected for multiple-scattering, for the different seasons (top) and for SVC, thin and opaque cirrus (bottom) are shown. Error bars indicate the counting statistics uncertainty.

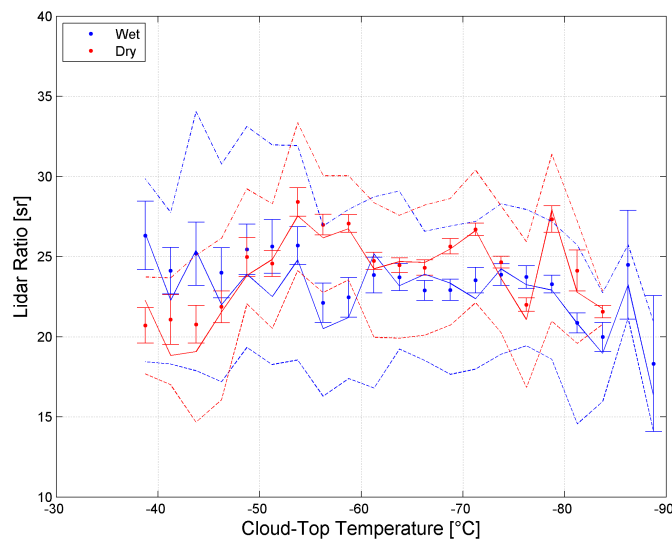


Figure 9. Dependence of the corrected lidar ratio with cloud-top temperature is shown for the wet (blue) and dry (red) seasons. The markers give mean and standard deviation of the mean. The continuous and dashed lines give median and interquartile distance. Temperature is divided in 2.5 °C intervals.

Unknown

Formatted: Font:(Default) Times New Roman, 10 pt